IEEE Access
Multidisciplinary | Rapid Review | Open Access Journal

Received January 16, 2017, accepted February 18, 2017, date of publication March 1, 2017, date of current version March 28, 2017.

Digital Object Identifier 10.1109/ACCESS.2017.2675625

Sensor-Less Predictive Drying Control of Pneumatic Conveying Batch Dryers

BIPLAB SATPATI[1], CHIRANJIB KOLEY[2], (Member, IEEE), and SUBHASHIS DATTA[3]

[1]Department of Electrical Engineering, University Institute of Technology, The University of Burdwan 713104, India
[2]Department of Electrical Engineering, National Institute of Technology, Durgapur 713209, India
[3]Department of Mechanical Engineering, Ghani Khan Choudhury Institute of Engineering and Technology, Malda 732102, India

Corresponding author: B. Satpati (biplabsatpati@yahoo.co.in)

This work was supported by the Department of Science and Technology, Government of West Bengal under Grant 321(Sanc.)/ST/P/S&T/6G1/2010).

ABSTRACT This paper presents predictive drying control design for a lab-scaled industrial pneumatic conveying dryer (PDC) involves with continuous/ batch processing of powder materials. The model predictive control (MPC) is an established method for drying control in various drying applications, such as fluidized bed dryers, rotary dryer, infrared dryer, timber dryers, baker's yeast dryers and so on. But the predictive control of PDCs have not been studied in the literature, however, these dryers are widely used in food, agriculture, and chemical industries, particularly suitable for batch processing of fine grained materials. The unavailability of any suitable control oriented first principle's model of these dryers make the predictive control design and implementation issues more challenging. Existing control methods for similar drying applications use outlet material moisture as a main control variable, online measurement, of which is difficult, costly, and unreliable due to the involvement of materials in granular/powder form. In the present contribution, an innovative control oriented model of the dryer is derived from first principle's encompassing a soft sensor-based online powder-moisture measurement procedure replacing the physical moisture sensors. The proposed physical sensor-less powder moisture control strategy stands on the traditional two-layer predictive control paradigm involving detection of an economically best operating point for batch dryer operation by optimizing the various process economic objectives followed by employing a suitable state space MPC (SSMPC) law for steering the process to operate at economically best operating point. The developed control strategy has been implemented and tested under practical settings and shown its effectiveness in improving the drying performance and product quality compared with an inbuilt auto-tuned proportional integral plus derivative controller of Honeywell make HC900 programmable logic controller.

INDEX TERMS Pneumatic conveying and drying process, first principle's model, heating and flow control process, parameterized gray-box nonlinear state-space model, state space model predictive control (SSMPC).

I. INTRODUCTION

The pneumatic conveying and drying technology has been extensively used in food processing and agricultural, chemical, polymer and ceramic, pharmaceutical, pulp and paper, and wood processing industries for removing the surface moisture of granular or fine grained (powder) materials with a particulate size of 10-500μm [1]–[4]. The pneumatic conveying continuous/batch dryers are highly preferred in aforementioned industrial processes because of various environmental, operational and economic benefits compared to the other dryers [1], [3], [4].

The main motivation for employing advanced control strategies in industrial drying is to produce products at a desired quality at maximum throughput, but at minimum cost [5]. In pneumatic convective drying inlet air temperature, initial moisture content, material throughput, relative humidity and velocity of the drying agent have a significant effect on the drying kinetics and product quality. Many flash dryers used in food, chemical, agricultural and pellet industries are still lean towards the manual (fixed gain PID's) control procedure for monitoring the drying conditions [1], [6], [7]. But this practice yields a poor energy efficiency, increased production costs and sometimes may degrade the product quality [5], [7]. Therefore, to achieve a satisfactory drying performance and processing the products as per desired quality, the inlet air temperature of the pneumatic conveying dryers require to be controlled dynamically according to the material throughputs and initial moisture content of wet materials. On the other

hand, flow rate needs to be governed in such a way so that the drying materials can attain a sustained conveyance and at the same time it ensures to provide an adequate drying time so that the material grains can get dried properly while conveyed through the vertical duct.

Moreover in pneumatic conveying dryers, the mass flow rate of the input raw materials, their initial moisture content, and their grain size often vary during operation, therefore the desired set points of the temperature and airflow controller needs to be dynamically altered according to the drying conditions. Unlike the relatively faster airflow control of the process, dryer inlet air-temperature control is more critical, because of the large time constants of the heating system employed and the dependency of the inlet air temperature on the airflow rate. Further, the different time constants at different operating region and involvement of various uncertainties and process nonlinearities make the existing PID control incompetent in providing a good disturbance rejection and an energy efficient operation particularly in the dynamically varying load situation [2], [4]. Thus to obtain a satisfactory drying performance, the drying controller has to be synthesized using model based control techniques [2]. There has been a significant number of research works on mathematical model of pneumatic conveying/flash dryer [8]–[13] based on first principle's, published in last two decades. These works highlight the formulation of complex transport equations based on partial differential equations (PDEs) aimed to either facilitate dryer design or obtain experimental and numerical solutions of some typical drying applications. But these models are not control-oriented and focused more on enhancing the design and qualitative aspects rather than the improving drying control mechanism. Apart from mathematical models, many knowledge-based models such as fuzzy-neuro rule based predictive models [14]–[17] genetic algorithm based models [4], [18], [19] and data driven black box models [20], [21] etc. of various dryers are also available in the literature. These models can offer detailed predictions of the fluid flow, heat & mass transfer and product quality. Moreover, in many drying applications, these models have been found suitable to employ the model based advanced control strategies for improving the drying performance [15], [19], [21]. Nevertheless, the control strategies stand on knowledge-based model suffers from certain disadvantages, such as performance of the control design using these models to a large extent depends upon initial data-set and operating conditions, outside the data-set performance is unknown and physical significance of the model parameters are very difficult to discern. Therefore to emulate the physical phenomena of drying system into the design, the knowledge–based data driven digital models should be supported by a suitable first principle's model. This is a most common practice in control engineering and successfully adopted in many applications. But the development of suitable control-oriented first principle's model of pneumatic conveying dryers is still under the scope of the research.

Over the past one decade the focus of drying control research has shifted from conventional PID control to model predictive control (MPC) approaches [6], [21]–[24]. There has been a notable number of research work on MPC design and implementation in the diverse application area of drying such as corn drying [25], timber drying [26], grain drying [27], [28], paper drying [29], [30], rotary dryer [24], [31], infrared drying process [21], [22], [32], drying in olive oil mill [31], [33], pasta drying [34], baker's yeast drying [15], [19] etc. In order to employ predictive control in aforementioned drying processes, the prevalent practice is to choose the material moisture as the main control variable. But the works contributed to this area have emphasized very less about the costs, difficulties and inaccuracies involved with the online measurement of solid moisture [3]. One of the most widely used sensors for online measurement of solid moisture is infrared moisture meter [35]. These sensors are accurate for local measurement, but infrared radiation fails to deeply penetrate the processing material; thus the measurement is superficial only [35]. Moreover, these sensors are highly expensive. Capacitive measurement is the relatively less expensive method for online measurement of product moisture but the measurement is inaccurate due to high noise variance during measurement. Related to online product moisture sensing, air humidity measurement in real time is also difficult, because this sensors are either inaccurate or have a short life span due to the harsh conditions present in a dryer [15], [31]. The difficulty of measuring solids moisture and air humidity in real time leads to an uncontrollable and unobservable drying process model, which makes control designing issues more challenging [3], [31], [35].

As an alternate to the physical sensors, many empirical rule, knowledge and model based estimation frameworks are available in the area of soft sensing [35]. Among the various approaches, the observer based soft sensor is the most prevalent, particularly in feedback control applications [36]. The observer based soft sensor provides an estimate of the unmeasured process variable from the measurement of input and output on the basis of a known dynamic model of the process. But to deal with the present application, finding an explicit dynamic model becomes challenging, because the values of many parameters of the first principle's model are difficult to determine from the physical dimensions, thermal and hydrodynamic properties and operational characteristics of the dryer and the processing material due to the high interdependencies among various parameters and the complex and distributed nature of the plant. Considering these complexities of observer based estimation an alternative framework has been employed in this contribution on the basis of a well-known temperature drop model [7], [37], [38] of the dryer and heat exchanger. The operating set point (dryer inlet air temperature and flow) for each batch of production are estimated by a soft sensor driven online set point estimator, which incorporates an estimator and an economic optimizer. At first the estimator computes a set of possible set points for a known drying condition of the processing material then an

Nomenclature

v_p= particle velocity (ms^{-1})	v_a= air velocity (ms^{-1})	C_d = drag coefficient (-)
f_p = frictional coefficient for the wall-particle interaction (-)	$A_p{}'$ = projected area of particle (m^2)	D_{pipe}= diameter of pipe(m)
f_a= Frictional Coefficient for the air-wall interaction (-)	ε = Volume fraction (m^3/m^3)	$\dot{w}$ = drying rate (Kg/m^{2}s)
ρ_a= air density (kgm^{-3})	ρ_p= particle density (Kgm^{-3})	g = gravitational Constant (ms^{-2})
$\Delta P_{blower,drop}$= total pressure drop in the blower (N/m^2)	P_1 = inlet conveying line pressure (static pressure at dryer inlet) (N/m^2)	P_2 = static pressure at blower inlet (N/m^2)
P_3 = static pressure at blower outlet (N/m^2)	P_4= static pressure at dryer exit (N/m^2)	C_p= specific heat of particle (J kg^{-1} K^{-1})
C_a= specific heat of air (J kg^{-1} K^{-1})	C_v= specific heat of vapor (J kg^{-1} K^{-1})	T_a= dryer inlet air temperature (K)
T_p= particle temperature (K)	T_{amb} = ambient temperature (K)	T_{a_0} = dryer outlet air temperature (K)
T_{pin} = material inlet temperature at hopper or rotary feeder (K)	T_{pout} = material outlet temperature at cyclone or collector (K)	ΔT = temperature drop between dryer inlet and outlet (log mean) (K)
T_{D_m}= dryer mean temperature (K)	$\dot{q}$ = heat in-flow per unit area (Wm^{-2})	ϱ = heat loss (W)
$\dot{m}_a$ = air flow rate (kg/s or kg/s/ m^2)	$\dot{m}_p$= particle (material) flow rate (kg/s or kg/s/ m^2)	ϕ = solid loading ratio (-)
h_{ap} = heat transfer coefficient air to particle (W/m^{2}K)	L= latent heat of vaporization (J/Kg)	τ = drying time (s)
M = material moisture in % on dry basis (Kg-water/Kg-dried solid)	M_0 = initial moisture content in % on dry basis (kg-water/kg-dried solid)	M_f = material final moisture in % on dry basis (Kg-water/Kg-dried solid)
$\Delta M = M_f - M_0$ = moisture to be removed in % on dry basis (kg-water/kg-dried solid)	H = absolute humidity of drying air (kg $_{\text{water vapor}}$/kg $_{\text{dry air}}$)	H_{ea} = relative humidity of air (*kg water vapor/kg dry air*)
S = production rate or dryer speed *(kg/s)*	ψ = blower flow (axial) coefficient (-)	N = speed of motor-blower drive (*rpm*)
v_{tip} = blower tip velocity (m/sec)	f = operating frequency of induction motor drive (*hz*)	D_{tip} = blower diameter (m)
T_{BW} = web-bulb temperature (K)	T_{AS} = adiabatic saturation temperature (K)	η_{T_max} = maximum thermal (energy) efficiency of the dryer (-)
ζ_1 and ζ_2= flow and temperature sensor's gain (-)	V_{avg} = average velocity of the air coming out of blower (m/s)	p = number of poles of induction motor (-)
A_{blower} = annular swept area of the blower (m^2)	Q = product quality *(%)*	Q_L= product quality loss (%)
s = operating slip of induction motor drive	u_1, u_2= control input (%)	
t_{dr}= disturbance recovery time (s)	e_{ss}= steady state accuracy *(-)*	J_a= energy cost of air *(kJ)*

optimal set point is obtained by optimizing the cost function including the indices such as operating cost, product quality loss etc. Thereafter the estimated optimal set point is used by the MPC control law to generate a set of manipulated inputs, which steers the process to operate at economically best operating point. Here the economic optimization is executed batch wise at a rate of hours/day (e.g. 4-6 hours interval for rice powder), but control action is taken in minutes/seconds (e.g. every 20 seconds for rice powder). A schematic block diagram of the proposed predictive control frame work is shown in Figure 1. The employed control strategy is most widely known as two-layer paradigm in process control literature. The paradigm has witnessed a numerous number of successful implementation, considering steady state economic operation of chemical processes [39]–[41].

However in very recent years, dynamic or time varying economic operation of chemical processes has attracted the attention of research community as well as industries. A new paradigm, Economic MPC (EMPC) is becoming very popular and effective in the context of chemical process operations [39]. In contrast with the traditional MPC, the EMPC method incorporates the process economics and process control objectives in a single cost function and which is optimized to operate the process in a possible time varying fashion.

In contrast with the traditional MPC, the EMPC method incorporates the process economics and process control objectives in a single cost function and which is optimized to operate the process in a possible time varying fashion. Though the present work deals with the traditional MPC framework, but it insights an important foundation work which can be extended for possible employment of EMPC in pneumatic conveying dryer.

The remainder of the paper is organized as follows: Section II describes about the experimental dryer setup, while in Section III, the background and theoretical framework of the present study related to the development of powder moisture soft sensor, first principle's model, closed-loop model identification in the structured form and state space MPC method are discussed. Section IV exemplifies the

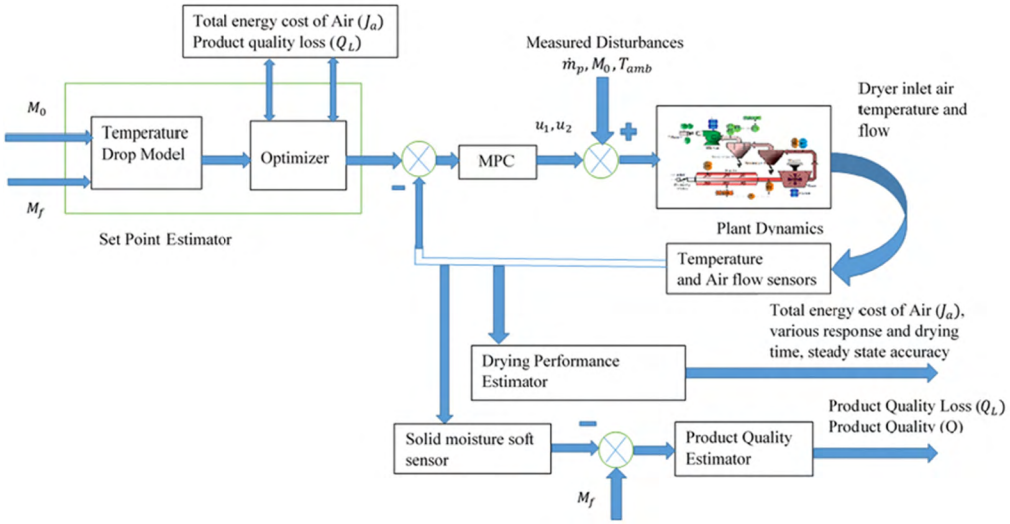

FIGURE 1. Schematic block diagram of the proposed predictive control framework.

experimental design and data collections procedure for batch processing of rice powder material, sought to carry out system identification and control design. Section V presents both results in simulation and in a real time application. The paper ends summarizing the contribution of the work in Section VI.

II. DESCRIPTION OF THE PROCESS

The process under investigation is a negative pressure closed-type lab-scaled pneumatic conveying system, which is particularly suitable for drying, conveying and separation of fine grained materials [2], [3]. The drying operation in these units is characterized by a coherent flow of a preheated gas–grain mix, where grains being de-hydrated or dried by the preheated air during transportation through the air duct, thereafter grains are separated according to size by some cyclone systems [2].

The schematic process flow and instrumentation diagram of the experimental set-up is illustrated in Figure 2, which consists of an air pre-heating furnace comprising a 1m inner diameter G.I. air duct fitted with six electrical heaters of 58 kW total heating capacity, a horizontal section consisting of a rotary feeder and mixing and grinding unit, a vertical pneumatic conveying duct (114.3 mm internal diameter and 1.8 m length), cyclone systems and a blower-IM motor drive (Maximum discharge 2548.5 m^3/h).

The heaters placed inside the preheating furnace are used to heat the drying air at desired temperature. The material to be processed is fed into the hopper and the feeding rate is being regulated by a rotary feeder. The vertical duct work is the main component of the dryer, which is used to convey the preheated air–grain mix in the upward direction caused due to the creation of a negative pressure zone inside the duct by means of a blower-motor drive, placed at end of the conveying line. *Resistance Temperature Detectors* (RTDs) are mounted on the duct in various locations to measure the air or air-grain mixture temperature. The dryer inlet air temperature is

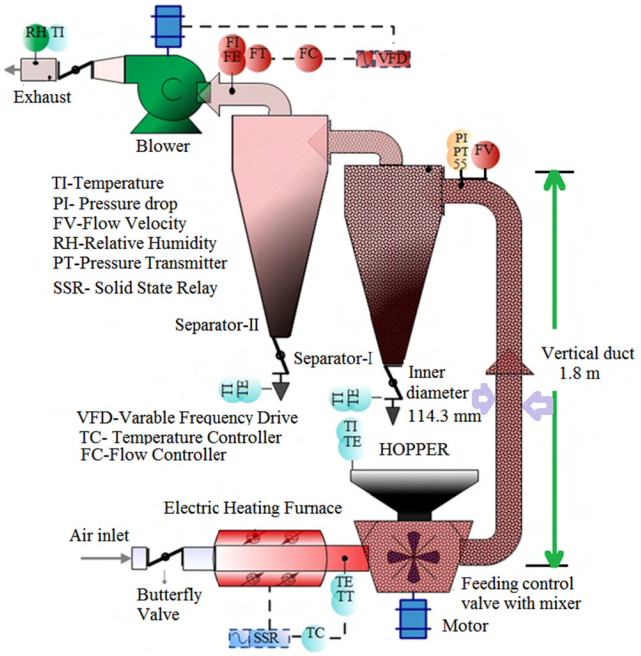

FIGURE 2. Process flow and instrument diagram.

measured by a RTD sensor placed prior to the rotary feeder and regulated by controlling the current through the heaters. In order to control the heater current, a 3-ph solid state relay (SSR) (model 25A, NIPONIX) is operated at high frequency in time proportional output (TPO) mode. The outlet air temperature and relative humidity of air are measured by relative humidity temperature meter (AMPROBE THDW-3) placed just prior to exit. The suspended powder material temperature in the cyclone systems are measured by infrared thermometer (emissivity 0.98). The airflow rate and pressure inside the duct are measured by v-cone (Mc-crometer) and

pressure transmitter (Honeywell, ST 3000) respectively, and is controlled by controlling the blower motor (3-ph induction type) through a variable frequency drive (VFD) (model IG5ASV015IG5A-4, LG).

Since the various control elements are distributed throughout the system, a Honeywell make HC 900 controller is used for monitoring and controlling the entire process. The outlet air temperature, airflow rate, and duct pressure are acquired by Analog Input (AI) channels of the HC 900 controller, and then sent to the respective PID controller, the output of the temperature PID controller is then sent to Digital Output (DO) port of the HC 900 controller through a TPO block, which then drive the SSR. The output of the airflow PID controller goes to the Analog Output (AO) port of the HC 900 controller, and then converted into 4-20 mA current output, which finally goes to the Variable Frequency Drive (VFD) for control of the blower speed. Initial and final moisture contents are measured using 10 g samples by an air-oven drying method (135 degree C for 24 h).

III. THEORETICAL BACKGROUND AND DEVELOPMENT

This section discusses the background and theoretical framework of the present study related to the development of material moisture soft sensor, control oriented first principle's model and structured model parameter identification technique from closed-loop experimental data. The section also gives a brief overview of the conventional state space model predictive control (SSMPC) design method, but the method has been modified as per the requirement of the control problem.

A. DEVELOPMENT OF SOLID MOISTURE SOFT SENSOR USING TEMPERATURE DROP MODEL

The solid moisture soft sensor developed in this section is a modification of the soft sensor model originally reported in [3]. In contrast to the earlier work, the temperature drop calculation steps of the presented model [3] have been reformed to a great extent by utilizing the concept of log-mean temperature difference of 1-1 co-current heat exchanger. The aforementioned modifications are incorporated in order to justify the model from theoretical standpoint.

In pneumatic conveying dryer the material moisture (M) at any appropriate point along the vertical duct during batch processing before the product leaves the dryer or collected by the cyclone system can be estimated from the measurements of product initial moisture (M_0), temperature drop between dryer inlet and outlet (ΔT) and production rate or dryer speed (S) [7], [42]. The model is based on the empirical rule,

$$M = M_0 + k_1 [\Delta T]^{\gamma} + \frac{k_2}{(S)^{\eta}}, \tag{1}$$

where k_1, k_2, γ and η are the empirical model constants depending upon the type, size and shape of the materials used for processing.

In the process under investigation the coherent flow of preheated gas–grain mix moves in the upward direction parallel to each other, therefore the vertical pneumatic conveying duct can be considered as 1-1 co-current heat exchanger. Considering the thermodynamic properties of co-current heat exchanger, the temperature drop between dryer inlet and outlet (ΔT) can be derived in terms of log-mean temperature difference [37], [38], given by

$$\Delta T = \frac{(T_a - T_{pin}) - (T_{a0} - T_{pout})}{ln\left(\frac{T_a - T_{pin}}{T_{a0} - T_{pout}}\right)} \tag{2}$$

The particle temperature at cyclone system or collector (T_{pout}) of pneumatic conveying dryer is obtained from the energy balance between drying agent and drying materials in dilute phase with the consideration of loss-less heat transfer [37], yields

$$T_{pout} = T_{pin} + \frac{\dot{m}_a c_a}{\dot{m}_p c_p}\left[T_a - T_{a_0}\right] \tag{3}$$

From the theoretical point of view of any adiabatic dryer, in order to operate the dryer near its maximum thermal efficiency (η_{T_max}), the dryer outlet air temperature (T_{a_0}) should be as close as possible to either the wet bulb temperature (T_{BW}) or the negligibly lower adiabatic saturation temperature (T_{AS}) [1]. On the other hand the drying materials are usually fed to the hopper at ambient temperature (T_{amb}).

Therefore without loss of any generality, it may be assumed:

$$T_{a_0} = T_{BW} = T_{AS} = T_a - \eta_{T\_max}\left[T_a - T_{amb}\right] \tag{4}$$

The production rate (S) of batch dryer proportionally varies with the material throughput or flow rate ($\dot{m}_p$).

Thus, using equations (2-4), the equation (1) is reshaped as follows:

$$M = M_0 + k_3 [T_a - T_{amb}]^{\gamma} + \frac{k_4}{(\dot{m}_p)^{\eta}}, \tag{5}$$

where $k_3 = \eta_{T\_max}\left(1 + \frac{c_a}{\phi c_p}\right) \Big/ ln\left(1 \Big/ \left(1 - \eta_{T\_max}\left(1 + \frac{c_a}{\phi c_p}\right)\right)\right)$ and k_4 is the modified proportionality constant.

Now for a given dryer dimensions, inlet conveying line pressure (P_1), dryer mean temperature (T_{D_m}) and conveying conditions, the minimum conveying air flow velocity ($v_{a_{min}}$), corresponding to the conveying limit can be determined by using the following equation [3], [4]

$$v_{a_{min}} = 0.1018 \frac{\dot{m}_p T_{D_m}}{Dpipe^2 P_1 \phi} \tag{6}$$

As addressed in the various literature of pneumatic conveying and drying [1], [3], [4] for dilute phase conveying the minimum conveying air flow velocity, $v_{a_{min}}$, will almost certainly be above 10 m/s to ensure that the material does not drop out of suspension and block the pipeline. The value of $v_{a_{min}}$ depends mainly upon mean particle size, particle shape and particle size distribution. This is typically in the region of 10–12 m/s for a very fine powder, to 14–16 m/s for a fine

granular material, and beyond for larger particles and higher density materials.

Design would generally be based on a conveying line inlet air velocity, v_a, 20 per cent greater than the minimum conveying air velocity [4]:

$$v_a = 1.2 v_{a_{min}} = 0.122 \frac{\dot{m}_p T_{D_m}}{D^2 P_1 \phi} \tag{7}$$

Therefore to get a sustained conveyance and meet the drying requirements, the constraints imposed on air flow velocity is given by

$$0.122 \frac{\dot{m}_p T_{D_m}}{D^2 P_1 \phi} < v_a < \frac{\Delta M}{\tau \left[H - H_{ea}\right]} \tag{8}$$

Now, Substituting $\dot{m}_p$ from (7) in (5), the desired material moisture (M_f) is estimated at the cyclone system before the product leaves the dryer, given by

$$M_f = M_0 + \mathrm{k}_3 \left[T_a - T_{amb}\right]^{\gamma} + k_5 v_a^{-\eta} \tag{9}$$

where k_5 is a model constant depending upon dryer geometry, particle properties, inlet conveying line pressure, dryer mean temperature and solid loading ratio.

B. FIRST PRINCIPLE's MODEL OF PNEUMATIC CONVEYING DRYER

The formulation of first principle's model is based upon momentum, energy and mass differential balances between drying agent and drying material with the consideration of one dimensional heat transport phenomena and dilute phase conveying for food particles as presented by Fyhr and Rasmuson [8], Tanaka *et al.* [11] and Plegrina and Crapiste [10]. In contrast with the existing models, the present contribution includes some necessary modifications to obtain control oriented mathematical model of pneumatic conveying dryer, taking into account the negative pressure conveying and complexities of online material moisture and air humidity measurement.

In order to develop controllable and observable state space model of pneumatic conveying dryer the unmeasured (measured offline) variables such as material moisture and air humidity were replaced in terms of measured process variables (dryer inlet air temperature and air flow rate) using temperature drop model. To facilitate control design pressure drop model of blower-motor drive has been incorporated and momentum balance differential equations were reshaped accordingly.

The first principl's model developed in this contribution primarily stands on some relevant assumptions as made by Fyhr and Rasmuson [8] and Plegrina and Crapiste [10], in addition with some application specific assumptions were also taken up such as:

1) *The model is developed by considering batch operation of pneumatic conveying dryer. Therefore, the particles having uniform shape (non-spherical) and size are fed during a batch of processing.*
2) *The throughputs* $(\dot{m}_p)$ *and initial moisture content* (M_0) *of material feeds can be varied or adjusted by the operator during a batch of production.*
3) *The solid loading ratio* (ϕ) *is kept constant for the entire batch of processing*
4) *Drag and heat transfer coefficients can vary with the shape and size of drying particles. Since uniform particles are fed in batch, therefore these coefficients can be assumed constant.*
5) *Sensor (temperature and flow) dynamics are ignored in the model, however sensor gains are considered.*
6) *Static air pressure drops in the conveying line are assumed to be equal at blower and dryer exits.*

Based on the above assumptions the process can be represented by the following set of equations (see Table I), which have been written in a suitable form for developing nonlinear state space model of pneumatic conveying dryer.

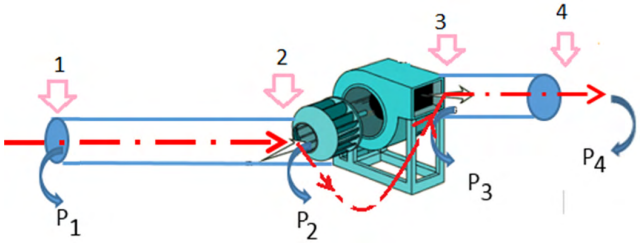

FIGURE 3. Schematic diagram of conveying line with motor blower drive.

Motor-Blower Dynamics: The process under investigation consists of a negative pressure conveying line, where the motor-blower drive is placed prior conveying line is shown in Figure 3. Here the static pressure of air has been considered in four different location of the conveying line *i.e.* P_1 at dryer inlet, P_2 at blower inlet, *and* P_3 at blower outlet and P_4 at dryer exit respectively (see the 'static pressure profile' presented by dashed-dot red line).

Through the conveying line, the air flow accelerates from position 1 to position 2 because of the static pressure drop generated at the entrance of the blower, and the static pressure drop at position 2 is equal to the dynamic pressure gain at that location.

$$\text{i.e. } P_1 = P_2 + \frac{1}{2}\rho_a v_{avg}^2 \tag{19}$$

The static pressure change across the blower is given by:

$$\Delta P_{blower,static} = P_3 - P_2 \tag{20}$$

Based on the *assumptions vi* ($P_3 = P_4$), the total static pressure drop created by the motor –blower drive in the conveying line can be determined as follows:

$$\begin{aligned} \Delta P_{blower,drop} &= P_2 - P_4 = P_1 - \frac{1}{2}\rho_a v_{avg}^2 - P_4 \\ &= -(P_4 - P_1) - \frac{1}{2}\rho_a v_{avg}^2 \\ &= -\Delta P_{static} - \frac{1}{2}\rho_{fan} v_{avg}^2 \end{aligned} \tag{21}$$

TABLE 1. Various balances and complementary equations of pneumatic conveying dryer.

Momentum balance equation [11], [10]		
Particle:	$\dot{v_p} = \frac{{A_p}'}{2Vol_p} C_d (v_a - v_p)^2 \frac{\rho_a}{\rho_p} - \left(1 - \frac{\rho_a}{\rho_p}\right) g - \frac{f_p}{2D_{pipe}} v_p^2$	(10)
Air:	$\dot{v_a} = \frac{1}{\rho_a v_a} \dot{\Delta P}_{blower,drop} - \frac{2}{D_{pipe}} f_a {v_a}^2 - g - \frac{{A_p}'}{2Vol_p} \left(\frac{1-\varepsilon}{\varepsilon}\right) C_d (v_a - v_p)^2 - \frac{{A_p}' \dot{w}}{\rho_a Vol_p} \left(\frac{1-\varepsilon}{\varepsilon}\right) (v_a - v_p)$	(11)
Energy balance equation [11], [10]		
Particle:	$\dot{T_p} = \frac{{A_p}'}{C_p \rho_p Vol_p} \left[h_{ap}(T_a - T_p) - \dot{w} L(T_p, M)\right]$	(12)
Air:	$\dot{T_a} = \frac{{A_p}'}{\rho_a C_a Vol_p} \left(\frac{1-\varepsilon}{\varepsilon}\right)(-\dot{q}) - \frac{\dot{q}}{\dot{m}_a C_a (1+H)} - \frac{\dot{w} {A_p}' C_v}{\rho_a C_a Vol_p} \left(\frac{1-\varepsilon}{\varepsilon}\right)(T_a - T_p)$	(13)
Mass balance equation [11]		
Particle:	$\dot{m}_p \frac{dM}{dt} = -\dot{m}_a \frac{dH}{dt}$	(14)
Air:	$\frac{dM}{dt} = -\frac{{A_p}'}{\rho_p Vol_p} \dot{w}(1 + M)$	(15)
Complementary equations		
Latent heat of evaporation in cereal grains or fine grained flour [43], [44], [45], [1]	$L(T_p, M) = \left[(k_6 - k_7 T_p)(1 + \alpha e^{-\beta M})\right]$, where k_6,k_7, α and β are system constant depending upon thermodynamic and physical properties of drying material.	(16)
Volume fraction: [11]	$\frac{1-\varepsilon}{\varepsilon} = \frac{\rho_a v_a \dot{m}_p (1+M)}{\rho_p v_p \dot{m}_a (1+H)}$	(17)
Drying rate: [11]	$\dot{w} = -\frac{\rho_p Vol_p}{{A_p}'} \frac{M}{1+M}$	(18)

Considering the axial flow and blower properties, the pressure drop calculated in (21) can be rewritten in the following form [46]:

$$\Delta P_{blower,drop} = -\frac{1}{2}\rho_a v_{tip}^2 \psi - \frac{1}{2}\rho_a \left(\frac{\dot{V}}{A_{blower}}\right)^2, \tag{22}$$

where the blower tip velocity

$$v_{tip} = \pi D_{tip} \frac{N}{60} \tag{23}$$

and V_{avg} is the volumetric air flow rate ($\dot{V}$) per unit annular swept area of the blower (A_{blower}).

Now for a uniform cross-sectional circular conveying duct volumetric air flow rate ($\dot{V}$) is proportionally varies with the air flow velocity (v_a). Therefore, (22) can be revised as follows:

$$\Delta P_{blower,drop} = -\frac{1}{2}\rho_a v_{tip}^2 \psi - \frac{1}{2} k_8 \rho_a \left(\frac{v_a}{A_{blower}}\right)^2, \tag{24}$$

where k_8 is a system constant and its value depends upon dryer geometry.

The axial flow coefficients ψ can be obtained experimentally and given by [46]:

$$\psi = \frac{\Delta P_{static}}{\frac{1}{2}\rho_{fan}(\pi D_{tip})^2 \left[2f\ (1-s)\ /p\right]} \tag{25}$$

Substituting (23) in (24), results in

$$\Delta P_{blower,drop} = -\frac{1}{2}\rho_a (\pi D_{tip})^2 \left(\frac{N}{60}\right)^2 \psi - \frac{1}{2} k_8 \rho_a \left(\frac{v_a}{A_{blower}}\right)^2 \tag{26}$$

Drying air humidity (H) and volume fraction $\left(\frac{1-\varepsilon}{\varepsilon}\right)$ calculations using Temperature Drop Model

In the preceding section the particle moisture (M) at any appropriate point along or inside the batch dryer has been estimated using temperature drop model and given by (5). Now using (5) and (14), the air humidity can be obtained as follows:

$$H = -\phi \left[M_0 + k_3 \left[T_a - T_{amb}\right]^{\gamma} + \frac{k_4}{(\dot{m}_p)^{\eta}}\right] + \aleph, \tag{27}$$

where $\aleph$ is a system constant.

In order to replace particle moisture (M) and drying air humidity (H) in the expression of volume fraction $\left(\frac{1-\varepsilon}{\varepsilon}\right)$, M and H obtained using (5) and (27) are substituted in (17)

and finally volume fraction is obtained as follows:

$$\frac{1-\varepsilon}{\varepsilon}=\phi\frac{\rho_a v_a\left[1+M_0+k_3\left[T_a-T_{amb}\right]^{\gamma}+\frac{k_4}{(\dot{m}_p)^{\eta}}\right]}{\rho_p v_p\left[1-\phi\left[M_0+k_3\left[T_a-T_{amb}\right]^{\gamma}+\frac{k_4}{(\dot{m}_p)^{\eta}}\right]+\aleph\right]} \tag{28}$$

Nonlinear State Space Model: The pneumatic conveying dryer is initially modeled with the four ordinary differential equations based on momentum and energy balances of particle and air as presented in (10)-(13). Then the dependent variables in the right hand side expression of (10)-(13) such as blower pressure drop (ΔP_{drop}), volume fraction $\left(\frac{1-\varepsilon}{\varepsilon}\right)$, drying rate ($\dot{w}$), latent heat of vaporization ($L\left(T_p, M\right)$), particle moisture (M) and drying air humidity (H) are substituted using (26), (28), (18), (16), (5) and (27) respectively, as applicable. Finally the first order vector matrix equations of the nonlinear process model are obtained (see Appendix-I) and the system is represented in the following form:

$$\dot{x}=f(x,u,d)\quad y=h\left(x\right) \tag{29}$$

where $x \in \mathrm{X} \subseteq \mathbb{R}^{n_x}$ is the state vector, $u \in U \subset \mathbb{R}^{n_u}$, and $d \in D \subset \mathbb{R}^{n_d}$ are the control and disturbance input vector respectively, $f\ (x, u, d)$ is the input and state dependent function vector of the state equation, $h(x)$ is the output function vector. The control inputs to the pneumatic conveying system are N the rotational speed of blower and $\dot{q}$ the heat input rate to the heaters. Along with the input variables, three disturbance inputs are also considered such as material inlet temperature (T_{amb}), material throughputs or flow rate $\left(\dot{m_p}\right)$ and initial moisture content of material (M_0). These variable strongly effects system operation and performance. The air flow velocity (v_a) and air temperature (T_a) are considered as output variables. The state variables of the process are chosen as air flow velocity (v_a), particle velocity (v_p), air temperature (T_a) and particle temperature (T_p), i.e.

$$\begin{aligned}
&v_a=x_1, v_p=x_2, T_a=x_3, T_p=x_4,\\
&N=u_1, \dot{q}=u_2, T_{amb}=d_1,\\
&\dot{m_p}=d_2, M_0=d_3, v_a=y_1 \text{ and } T_a=y_2, \text{ where}\\
&x=[x_1,x_2,x_3,x_4]^T, U=[u_1,u_2,d_1,d_2,d_3]^T \text{ and}\\
&y=[y_1,y_2]^T.
\end{aligned} \tag{30}$$

By rearranging the first order vector matrix equations in the structure as presented in (29) with the consideration of (30), the following state space model is obtained:

State equation :

$$\dot{x}=f\ (x,u,d)=\begin{cases} f_1\ (x_1,x_2,x_3,u_1,d_1,d_2,d_3)\\ f_2\ (x_1,x_2)\\ f_3(x_1,x_2,x_3,x_4,u_2,d_1,d_2,d_3)\\ f_4\ (x_3,x_4,d_1,d_2,d_3)\end{cases}$$

Output equation : $y=h\left(x\right)=\begin{cases} h_1\ (x_1)=\zeta_1 x_1\\ h_1\ (x_3)=\zeta_2 x_3\end{cases}$ (31)

Linearization of State Space Model: The nonlinear model of pneumatic conveying and drying process is linearized about a selected operating point, chosen on the basis of a suitable drying condition ($\mathrm{M_f}$, $\mathrm{M_0}$, $\Delta\mathrm{M}$) considering the thermal and hydrodynamic properties of dryer and physical properties of the processing powder material, to ease the control design and implementation issues.

To linearize the model (31), the Taylor series method is used. In developing this linearization, it is assumed that all process variables have their respective values in the vicinity of a selected drying condition (operating point), which is denoted in the following by the index "o"; i.e. $\mathrm{x}=\mathrm{x_o}+\Delta\mathrm{x}, \mathrm{y}=\mathrm{y_o}+\Delta\mathrm{y}, \mathrm{u}=\mathrm{u_o}+\Delta\mathrm{u}, d=d_0+\Delta d$. In order to approximate the nonlinear state equations only the first-order derivative elements in the Taylor series are taken into account. Applying Taylor series in (31) and in accordance with the assumptions above, the linearized state space model of the process is obtained as follows:

$$\begin{aligned}
\Delta\dot{x}&=A\Delta x+B_u\Delta u+B_d\Delta d\\
\Delta y&=C\Delta x,
\end{aligned} \tag{32}$$

where $\mathrm{A}=\frac{\partial f(x,u,d)}{\partial \mathrm{x}}|_{\mathrm{x_o},u_o,d_0}$, $B_{u/d}=\frac{\partial f(x,u,d)}{\partial u/d}|_{\mathrm{x_o},u_o,d_0}$ and $C=\frac{\partial h(x)}{\partial \mathrm{x}}|_{\mathrm{x_o}}$

C. CONTROL RELEVANT IDENTIFICATION

The state space model of pneumatic conveying dryer derived from first principle's model contains many physical parameters and system constants. The state space model to be identified through system identification in accordance with the structures as derived in (32), which can be rewritten in the discrete state spaceform by discretizing the system at a sampling rate of T as follows:

$$\Delta x\ (k+1)=A_\theta\Delta x\ (k)+B_{u_\theta}\Delta u\ (k)+B_{d_\theta}\Delta d(k) \tag{33}$$

$$\Delta y\ (k)=C_\theta\Delta x\ (k)\,, \tag{34}$$

Where $\Delta x\ (k)$ is (4×1) state vector, $\Delta u\ (k)$ is (2×1) control input vector, Δy(k) is (2×1) system output vector and $\Delta d(k)$ is (3×1) measured plant input disturbance vector, A_θ, B_{u_θ}, B_{d_θ} and C_θ are system input-coupled matrices corresponds to control input vector and measured plant input disturbance vector and output-coupled matrices respectively of appropriate sizes parameterized by a set of parameters θ.

Everywhere $\theta := [\theta_1, \theta_2, \theta_3, \ldots\ \ldots., \theta_{24}]^T$, transformed parametric space $'\Omega : \left\{\theta : \theta \in \mathbb{R}^{24}\right\}$,

$$A_\theta=\begin{bmatrix}\theta_1&\theta_2&\theta_3&0\\ \theta_4&\theta_5&0&0\\ \theta_6&\theta_7&\theta_8&\theta_9\\ 0&0&\theta_{10}&\theta_{11}\end{bmatrix},$$

$$B_\theta=\left[B_{u_\theta}B_{d_\theta}\right]=\begin{bmatrix}\theta_{12}&0&\theta_{13}&\theta_{14}&\theta_{15}\\ 0&0&0&0&0\\ 0&\theta_{16}&\theta_{17}&\theta_{18}&\theta_{19}\\ 0&0&\theta_{20}&\theta_{21}&\theta_{22}\end{bmatrix}$$

$$C_\theta=\begin{bmatrix}\theta_{23}&0&0&0\\ 0&0&\theta_{24}&0\end{bmatrix} \tag{35}$$

In order to estimate parameters of the model presented in (33-35), the structured parameterization of state space matrices A_θ, B_{u_θ} and C_θ is our primary concern, as because the structure of the linear time invariant (LTI) state-space model has been deduced from physical considerations and the operating conditions. Thus, the system identification technique to be employed should have the ability to handle gray-box LTI structured parameter identification problem.

Among the various system identification techniques, subspace based approaches are most common for identifying the parameters of black-box (fully parameterized) LTI state space model. These methods are non-iterative, highly computationally intensive and well suited for both open and closed-loop identifications [47], [48]. But the appropriateness of the subspace based identification methods drops radically when gray-box state space models are considered [49], [50]. Predictions or output error based frameworks are the good substitute of subspace based approaches, often used in black-box LTI state space model identifications. But if these methods are adopted for gray-box state space model identification, success of the estimation to a large extent depends upon the selection of optimizer and initial parameter vector, wrong initialization of parameter vector may lead to the rise of local minima issues [50]. As an alternative to the conventional frameworks, many researchers have been employed a two- or three-steps iterative framework [49], [51] for identifying the parameters of gray-box state space model. First, an initial fully parameterized black-box model is estimated in state space from using subspace methods, then the initial black-box model has been transformed into gray-box form, either by enforcing some parameters to zero or replacing by known values as per the desired structure. The initial model obtained in structured form is further used as an initial model of a prediction error based recursive estimation algorithm to identify the parameters as per the desired structures. Nevertheless, the success of the estimation through iterative algorithm is subjected to accuracy of initial parameter values and efficiency of the designer [49]. In order to avoid the iterative algorithm and address initial model issues, polynomial optimization or numerically reliable approach has been employed by few researchers. Still the applicability of these methods is limited to small size models.

Apart from the model structure, the collection of identification data is another important concern. It is established for model based control design; closed-loop identification gives better performance [52]. However, closed-loop identification presents some additional complications for system identification. The fundamental problem is the controller induced correlation between the output noise and the plant input through the feedback. Because of this correlation, many conventional identification methods such as least squares estimate method, maximum likelihood method, empirical transfer function estimation, instrumental variable methods etc. may yield a large estimation bias, and even lead to unidentified model [53], [54]. Nevertheless, a significant number of methods generally based on subspace identification [48], [55] or stochastic based search algorithm [56], [57] have been found very effective for closed-loop identifications. Particle swarm optimization (PSO) [58] is one of the most widely used intelligent computational methods based on stochastic searchfor identifying the process model. In many applications, PSO based stochastic search algorithms were found to be very accurate for structured model estimation in gray-box form [59]–[61]. Though, most of the researches conducted in this area were used for open loop identification data. Therefore the applicability and closed-loop identification problem formulation of PSO based stochastic search algorithms are still under the scope of research.

The present paper uses a refined PSO based stochastic search framework to develop a closed-loop structured model parameter estimation method. The estimation algorithm is being improved greatly by considering some adaptive modifications in the penalty functions (adaptive penalty function) [62] involved with the least squared constraint optimization problem.

Closed-Loop Refined-PSO Based Stochastic Search Framework for Structured Model Parameters Identification: Consider the perturbed system represented by set of equations (33-35). The system has an existing set of proportional controllers (temperature and flow PIDs, both operating in proportional mode) placed in the forward path with a gain matrix $G = \begin{bmatrix} G_{11} & 0 \\ 0 & G_{22} \end{bmatrix}$.

In contrast to the experiments performed for the purpose of identification, an additional excitation/noise input $\Delta v(k)$ is injected to the control input, and the total input to the closed-loop system become

$$\Delta u\,(k) = G\,[\Delta r\,(k) - \Delta y\,(k)] + \Delta v(k), \tag{36}$$

where $\Delta u\,(k) = \begin{bmatrix} \Delta u_1(k) \\ \Delta u_2(k) \end{bmatrix}$, $\Delta r\,(k) = \begin{bmatrix} \Delta r_1(k) \\ \Delta r_2(k) \end{bmatrix}$, $\Delta y\,(k) = \begin{bmatrix} \Delta y_1(k) \\ \Delta y_2(k) \end{bmatrix}$ and $\Delta v\,(k) = \begin{bmatrix} \Delta v_1(k) \\ \Delta v_2(k) \end{bmatrix}$, which yields the following closed-loop system (perturbed) of the form

$$\Delta x\,(k+1) = \widehat{A_\theta}\Delta x\,(k) + \widehat{B_{u_\theta}}\Delta r\,(k) + \widehat{B_{d_\theta}}\Delta w\,(k) \tag{37}$$

$$\Delta y\,(k) = \widehat{C_\theta}\Delta x\,(k)\,, \tag{38}$$

where $\widehat{A_\theta}$, denotes the closed-loop system matrix, $\widehat{A_\theta} = A_\theta - B_{u_\theta}GC\,(\theta)$, $\widehat{B_{u_\theta}}$, designates the closed-loop input-coupled matrix corresponds to reference signal $\Delta r\,(k)$, $\widehat{B_{u_\theta}} = B_{u_\theta}G$, $\widehat{B_{d_\theta}}$ signifies the closed-loop input-coupled matrix corresponds to dither signal $\Delta w\,(k)$, $\widehat{B_{d_\theta}} = \left[B_{u_\theta}; B_{d_\theta}\right]$ and $\Delta w\,(k) = [\Delta d\,(k)\,; \Delta v(k)]$,

$\widehat{C_\theta}$ denotes the closed-loop output coupled matrix, $\widehat{C_\theta} = C_\theta$.

The objective of the problem is to obtain a state space model of the open-loop system, denoted by the set A_θ, $B_\theta = \left[B_{u_\theta}B_{d_\theta}\right]$, C_θ from the known closed-loop data set $[\Delta r\,(k)\,, \Delta w\,(k)\,, \Delta y\,(k)]$ and controller G.

The identification problem is formulated in terms of an optimization problem in which the error between an actual

physical measured response of the system and the simulated response of a parameterized model is minimized.

The objective function defined as the weighted mean squared errors between measured and simulated responses for a number N of given samples is considered as fitness of estimated model parameters:

$$J_{obj} = \frac{1}{N}\left[\sum_{i=1}^{N} \beta_1 (y_{i1m} - \widehat{y}_{i1sim})^2 + \beta_2 (y_{i2m} - \widehat{y}_{i2sim})^2\right] = \frac{1}{N}\left[(y_{1m} - \widehat{y}_{1s})^T \bar{Q}_1 (y_{1m} - \widehat{y}_{i1s}) + (y_{2m} - \widehat{y}_{2s})^T \bar{Q}_2 (y_{2m} - \widehat{y}_{2s})\right], \quad (39)$$

where y_{1m}, y_{2m} and $\widehat{y}_{1s}$, $\widehat{y}_{2s}$ are measured and simulated outputs, β_1, β_2 are the death penalty values ($\beta_1, \beta_2 > 0$) and $\bar{Q}_1$ and $\bar{Q}_2$ are the scalar weighting matrices given by $\beta_1 eye\,(N, N)$ and $\beta_2 eye\,(N, N)$ respectively.

In defining the objective function (J_{obj}) for stochastic based search algorithm many researchers used death or static penalties [63], [64]. But the death penalty function sometimes leads to infeasible solutions if the weights are too small or very poor quality solutions if the weights are too high. Therefore to minimize the possibility of finding infeasible and poor quality solutions in the search space, death penalty values β_1 and β_2 are modified by adopting adaptive penalty functions [62].

Particle Position, Velocity and Weight Update Equations in PSO Algorithm: PSO is a nature inspired algorithm based optimization tool, which was developed by Kennedy [58] motivated by the social behavior of bird flocking and fish schooling. Kennedy demonstrated that the velocity and position of the particles can be updated as follows:

Velocity Update:

$$V_i^{t+1} = WV_i^t + \kappa_1 rand_1 \left(X_{Pbest} - X_i^t\right) + \kappa_2 rand_2 \left(X_{gbest} - X_i^t\right) \quad (40)$$

Position Update:

$$X_i^{t+1} = X_i^t + \gamma V_i^{t+1} \quad (41)$$

Where κ_1 and κ_2 are two positive constants, $rand_1$ and $rand_2$ are random numbers in the range of [0, 1], W is the inertia weight, X_i^t represents current position of i^{th} particle, V_i^t represents current velocity, X_{Pbest} and X_{gbest} represents local and global best position of the particles receptively. The position of the particles are updated using equation (41), where X_i^{t+1} is the new position of the particle in the search space.

Weight Update: The weight W is updated as follows:

$$W = W_{max} - \left[\frac{W_{max} - W_{min}}{iter_{max}}\right] iter, \quad (42)$$

where *iter* is the iteration count.

Adaptive Penalty Modifications: In adaptive penalty method, the weights β_1 and β_2 are updated for every j iterations according to information collected from population. The penalty functions β_1 and β_2 are updated for every j iterations as follows [2], [62]:

$$\beta_{1\,or\,2}(t+1) = \begin{cases} \frac{1}{\Gamma_1}\beta_{1\,or\,2}(t) & \textit{if all the best particle in the last } j \textit{ iterations are feasible} \\ \Gamma_2 \beta_{1\,or\,2}(t) & \textit{if they are not feasible} \\ \beta_{1\,or\,2}(t) & \textit{otherwise} \end{cases} \quad (43)$$

It indicates, if all best particles of last j iterations are feasible, penalty term $\beta_{1\,or\,2}(t+1)$ for iteration $(t+1)$ decreases. If they are unfeasible, the penalty term is increased. Otherwise if the best individuals in the last j iterations consist of feasible and unfeasible solutions, the penalty term does not change. Γ_1 and Γ_2 are the scaling factors and $\Gamma_1, \Gamma_2 > 1$, $\Gamma_1 > \Gamma_2$ and $\Gamma_1 \neq \Gamma_2$.

Identification Algorithm: The identification algorithm integrates the considerations for closed-loop estimation, particle swarm optimization and adaptive penalty function method. The identification algorithm involves the following steps:

Step 1: Load the closed-loop experimental data set $r(k), w(k), y(k)]$, also specify the data size N and controller gain G.

Step 2: Determine the parameters to identify, define the model structure and matrices $A_\theta, B_{u_\theta}, B_{d_\theta}$ and C_θ as presented in (35).

Step3: Initialize a population of $\boldsymbol{g}$ particles with random positions within the lower and upper bound of the problem space. Similarly initialize randomly $\boldsymbol{g}$ velocities associated with the particles. The dimension of the search space must be same as the number of parameters to be identified. Also specify the maximum number of iteration.

Step 4: Initialize the state vector as $x(0) = \begin{bmatrix} 0 & 0 & 0 & 0 \end{bmatrix}^T$ and $y_{sim} = \begin{bmatrix} 0 & 0 \end{bmatrix}^T$

Step 5: Initialize the initial weight of the penalties β_1 and β_2 and scaling factor Γ_1, Γ_2 such that, $\Gamma_2 > 1$, $\Gamma_1 > \Gamma_2$ and $\Gamma_1 \neq \Gamma_2$.

Step 6: Compute the closed-loop model matrices $\widehat{A_\theta}, \widehat{B_{u_\theta}}, \widehat{B_{d_\theta}}$ *and* $\widehat{C_\theta}$ for the initial population.

Step 7: Calculate $y_{sim}(i)$ and $x(i+1)$ using (38) and (37) for the entire experimental data set *i.e.,* $i = 1{:}\, N-1$.

Step 10: Evaluate the optimization fitness functions J_{obj} for the initial population using (39).

Step 11: Find the minimum fitness value for fitness functions J_{obj} in **Step 10** and call it J_{Pbest} and let the particle associated with it be X_i.

Step 12: Initially set J_{gbest} equal to J_{Pbest}.

Step 13: Update the particle weight W using (42).

Step 14: Update the velocity of each particle using (40). Check V for the range [*Vmax, Vmin*]. If not, set it to the limiting values.

Step 15: Update the position of each particle using (41), which gives the new population.

Step 16: Compute the closed-loop model matrices $\widehat{A_\theta}$, $\widehat{B_{u_\theta}}, \widehat{B_{d_\theta}}$ *and* $\widehat{C_\theta}$ for the new population

Step 17: Repeat ***Step 7*** for the new population.

Step 18: Evaluate the optimization fitness functions J_{obj} for the new population using (39).
Step 19: Obtain new J_{Pbest} for fitness functions J_{obj} for new population.
Step 20: Compare the J_{Pbest} obtained in step 19 with J_{gbest}. If J_{Pbest} is better than J_{gbest} then set J_{gbest} to J_{Pbest}.
Step 21: Check the iteration count. If iteration count $=j$ check the fitness values of J_{Pbest} for the last j iterations, *else go to* ***Step 13***.
Step 22: Updatepenalties β_1 and β_2 using (43).
Step 23: Modify the objective function J_{obj} using (39) and *go to* ***Step 13***.
Step 24: Check the convergence criteria (maximum number of iteration, fitness value). If met exit the iteratio; otherwise return to ***Step 13*** and update iteration count by one.

D. CONTROL DESIGN

The anticipative temperature and flow control law employed in the present contribution uses the conventional constrained state space model predictive control approach (SSMPC), which has been attracted an increasing attention of a significant number of researchers over the last few decades, in order to handle some complex industrial control problems [65]–[68]. In the process under investigation, the main concerns of performing control design are reducing energy consumption and improving product quality, which can be obtained by maintaining a desired temperature and flow profile of drying agent over the length of the dryer. To achieve the control objectives, the control strategy is transformed into Quadratic Programming (QP) problem where a quadratic objective function subject to linear inequality constraints is minimized online. In formulating the Constrained SSMPC problem for the present study, the future trajectory predictions were generated using the innovation bias approach, which is equivalent to carrying out predictions using the observer augmented with an artificially introduced integrated white noise model. The observer has been developed using a Kalman predictor [66]. The state estimation, prediction and optimization methods employed in control design has been discussed in details by Wang [65], Li *et al.* [66], and Mustapha *et al.* [68].

IV. EXPERIMENTAL DESIGN AND DATA COLLECTIONS

The choice of the excitation signal is a very important issue of concern before finding the suitable model of the multivariable process under observation. The system should be excited in such a way that all interesting areas of the input space and all relevant frequencies are covered. That is why amplitude modulated pseudo random binary signal (APRBS) [69] has been considered in designing the closed-loop experiments for system identification.Rice powder was used as a model drying material to carry out the experiments for system identificatio and hence the control design. Here the fine grained rice flour sample (mean diameter (d_{p0}) 95 μm) of Indian basmati (Basmati 370) [70] has been considered for experimental study. The moisture conditioning of rice powder was performed by adding pure water to the rice flour and keeping the wet sample inside a freezer within plastic bags for 24 hours. As per the requirement of identification, two different moisture conditioned samples were prepared. After the moisture conditioning the samples were kept at the room temperature approximately for two hours so that the materials could attain ambient temperature before placed in the hopper. The moisture content of samples were measured by an air-oven drying method. Before performing the tests the experimental setup was used to run for one hour under no-load to eliminate the startup effects. The test was repeated for three times in order to acquire more accurate data to perform the system identification and validation. Among the three sets of data, one randomly chosen set has been kept entirely separate for final validation purpose. The remaining two data sets have been used for model estimation and testing using a 2-fold cross-validation (cv) test, which is discussed in detail by Satpati *et al.* (2014) [2].

To formulate the data-driven model of the pneumatic conveying and drying process in closed-loop the following measures were taken during the experiments:

- *The temperature and flow PID controllers were kept in AUTO mode with P, I and D setting of PB=100%, Td=0 and Ti=infinite.*
- *Set point of temperature PID was varied in pseudo-random manner within 50-120°C.*
- *Set point of flow PID was varied in pseudo-random manner within 133.33 -328.35 m^3/h.*
- *Inlet material temperature was considered to be varied in accordance with the ambient temperature.*
- *Material was fed into the rotary feeder at a constant feeding rate of 20 $kg/s/m^2$ (per cross sectional area of the vertical duct) for a considerable duration thereafter feeding rate has been changed to 25 $kg/s/m^2$ for next duration.*
- *During the experiments, two different moisture conditioned (27.27% and 29.7%) rice powder samples were used, the samples were fed into the rotary feeder one after another, i.e. 27.27% moisture conditioned sample approximately for first three hours and second sample for next couple of hours duration.*
- *Loop rate of the DCS was set to 1 Hz.*
- *The heat energy supplied to the heater coil (Q) was computed by transforming the measured current data. The heater current was estimated from the TPO-duty cycle of PLC, which generates a PWM signal to operate the SSR connected with the heating coil. Thus the error involved in the measurement of current was significantly low.*
- *The mixing motor was used to rotate at constant speed during all the experiments.*

V. RESULTS AND DISCUSSIONS

The obtained results, grouped in two categories are presented in the following subsections. These are the *model estimation and validation* and *control design*.

TABLE 2. Physical parameters of first principle's model.

Parameters	Values
Mean diameter of particle (d_{p0})	95 μm
Projected area of particle ($A_p{}'$)	5.67×10^{-8} m^2
Particle volume (Vol_p)	3.59×10^{-12} m^3
Particle surface area per unit particle volume (a_v)	6.3×10^{4} m^{-1}
Density of air (ρ_a)	1.225 kg/m^3
Diameter of the duct (D_{pipe})	0.1143 m
Material throughput ($\dot{m}_p$)	*20 kg/s/m^2*
Absolute humidity of air (H_0)	0.009 kg/kg-dried air
Initial material moisture (M_0)	0.2727 kg-water/kg-dried solids
Ambient Temperature (T_{Amb})	$30.39^{\circ}C$
Mean dryer temperature (T_{Dm})	$85^{0}C$
Solid loading ratio (ϕ)	3.9

TABLE 3. PSO and Objective function parameters.

Parameters	values
Maximum Iteration	1500
Population Size	100
Dimension	24
Value of κ_1, κ_2	2
γ	0.5
Maximum Weight	0.95
Minimum Weight	0.2
Number of data points (N) (2-fold cv data set)	21600, 18910
Gain matrix $G = \begin{bmatrix} G_{11} & 0 \\ 0 & G_{22} \end{bmatrix}$	$\begin{bmatrix} 1 & 0 \\ 0 & 1 \end{bmatrix}$
$v(k)$	Zero mean white noise (noise power 0.1)
Γ_1	100
Γ_2	10
j	20
β_1	1e8
β_2	9e7

A. MODEL ESTIMATION AND VALIDATION

The nonlinear state space model of the pneumatic conveying dryer derived from first principl's, has been linearized at a known drying condition i.e. initial moisture content $M_0 = 0.2727$ kg-water/kg-dried solids and final moisture content $M_f = 0.1256$ kg-water/kg-dried solids, then the structured model parameters of the linearized process have been identified using the proposed estimation method on the basis of identification data-sets (2-fold cv data set), collected from closed-loop experiments. The values of some of the physical parameters involve with the first principl's model are presented in Table 2. The control parameters of PSO algorithm and initial penalty values of objective function (39), as found to be suitable through hit and trial method are presented in Table 3.

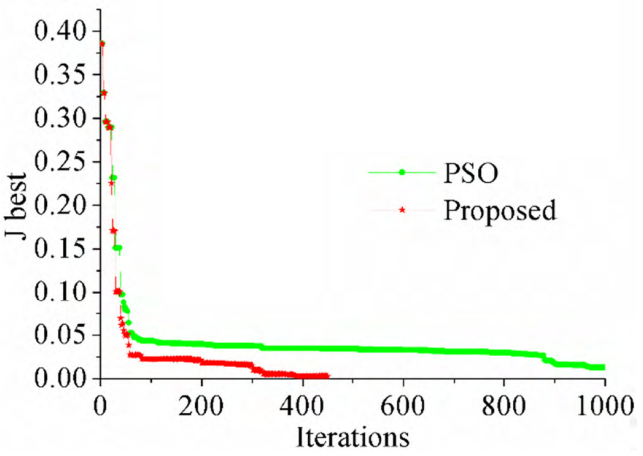

FIGURE 4. Comparison of convergence between proposed method and PSO.

The computational intensiveness and accuracy in parameter estimation are the main concern of any stochastic search based system identification algorithm. The convergence speed (number of iterations) is the measure of computational intensiveness and the accuracy in estimation is ascertained by the final fitness value of objective function. In order to verify the proficiency of proposed method over the conventional PSO based approaches, a comparative study has been carried out and depicted in Figure 4. The figure demonstrates, the conventional

PSO approach undergoes 1,053 performance evaluations to reach its best fitness value (0.01289), while the proposed method finds the much improved global optimum value (0.002787) in only 458 runs for the estimation data-set.The adaptive modifications in the penalty functions involved with the weighted least squared constraint optimization has reduced the computational time by approximately 57% compared to the conventional PSO based search method. The study also affirmed the benefits of blending adaptive penalty function method with the conventional PSO algorithm to create a more sophisticated and improved algorithm, particularly suitable for structured identification.

The state space model matrices of linearized pneumatic conveying dryer [A_θ, B_{u_θ}, B_{d_θ} and C_θ], estimated using proposed PSO algorithm with the help of identification data sets (2-fold cv data set), are presented in Appendix II.

A section of the final validation data-set, consisting of air flow and temperature set points ($r_1(k)$, $r_2(k)$), measured output ($y_{1m}(k)$, $y_{2m}(k)$), control inputs ($u_1(k)$, $u_2(k)$) and measured input disturbances ($d_1(k)$, $d_2(k)$, $d_3(k)$) are shown in Figure 5.

Plots of measured output data ($y_{1m}(k)$, $y_{2m}(k)$) and corresponding simulated output response ($y_{1sim}(k)$, $y_{2sim}(k)$) along with the set point signal is presented in Figure 5 panels a-b. The requisite control inputs ($u_1(k)$, $u_2(k)$) and measured input disturbances ($d_1(k)$, $d_2(k)$, $d_3(k)$) for closed-loop identification are plotted in Figure 5 panels c and d respectively. Figure 5.a shows the comparison for measured

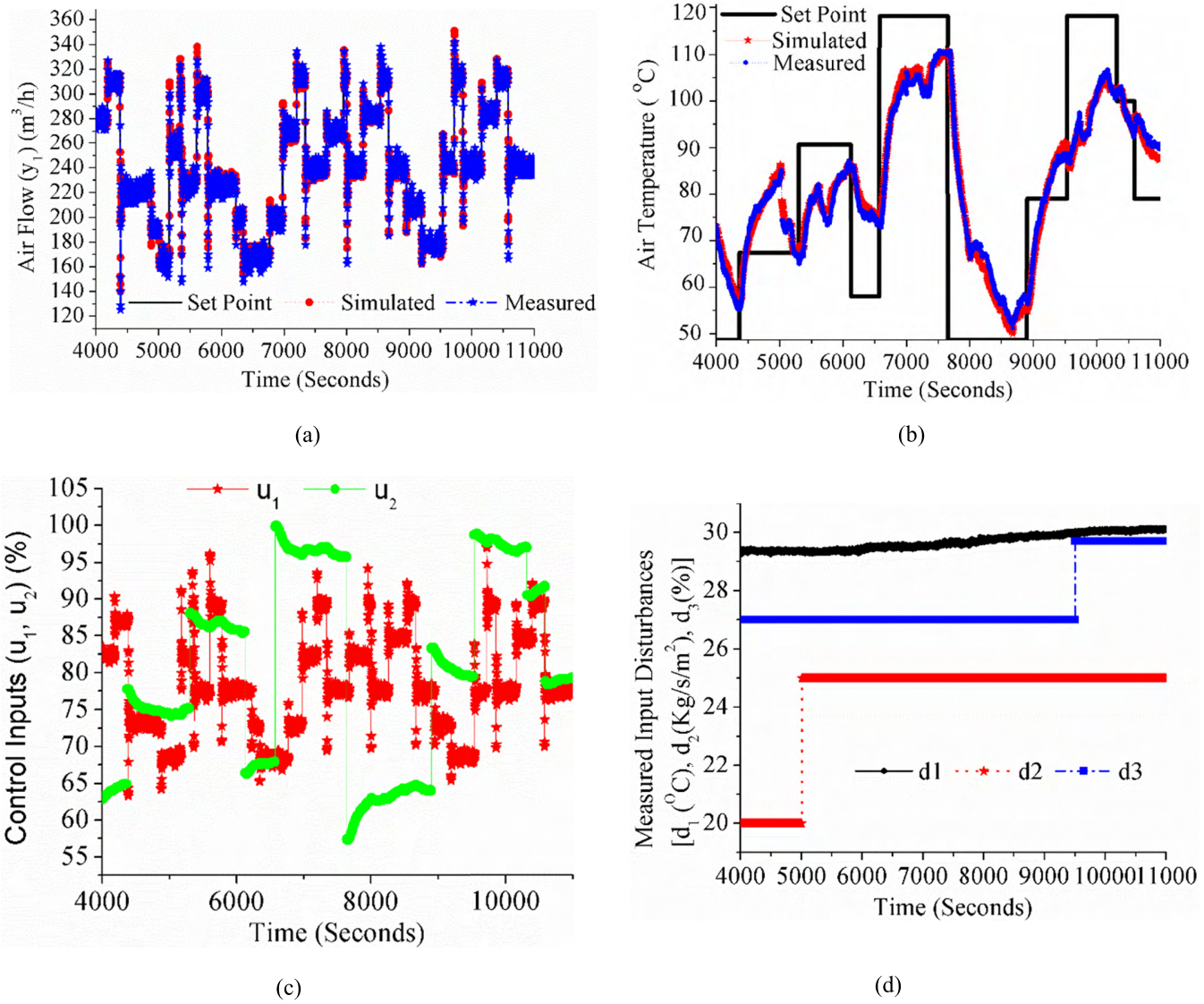

FIGURE 5. Plot of a) measured and simulated air flow (m^3/h) along with the flow set point b) measured and simulated air temperature (degree C) with corresponding set point c) control inputs u_1, u_2 (%) d) measured plant input disturbances d_1 (°C), d_2 (kg/s/m^2), d_3 (%).

and simulated air flow output in m^3/h and Figure 5.b shows the similar comparison for air temperature in $^\circ C$. It is evident from Figure 5 panels −d that the responses of the estimated models are closely correlated with the respective response of the actual process when various control and disturbance inputs are applied simultaneously.

Further, a step response test has been carried out to investigate the relevance of simulated model in reflecting the physical properties and characteristics of the real process. Figure 6.a depicts the step responses of the outputs air flow (y_1) and air temperature (y_2)) with respect to unit step changes in control inputs (u_1, u_2) and measured plant input disturbances (d_1) respectively. Similar kind of exercise has been performed for the rest of the transmittances and presented in Figure 6.b. It is seen from the figure, the air flow rate (y_1) of the dryer increases with the increase of blower speed (u_1) and remains almost invariant with change of heater current (u_1). On the other hand, air temperature (y_2) decreases with the increase of blower speed (u_1) and increases with increase of heater current input (u_2). The study also indicates, the process output responses are very much sensitive with respect to the variation of measured disturbance inputs such as material inlet temperature (d_1), material flow rate (d_2) and initial moisture content (d_3). However, the effect of material inlet temperature variation on air flow response is insignificant. It is evident from the figure, the output responses interacted with various control and disturbance inputs involve with the different time constants, which have physical meaning.

In order to determine the accuracy in estimation, the statistical attribute coefficient-of-determination R_T^2) has been considered, which is defined as [Satpati *et al.* [2]]

$$R_T^2 = \left[1 - \frac{\|y_m - y_{sim}\|_2^2}{\|y_m - \bar{y_m}\|_2^2}\right], \tag{44}$$

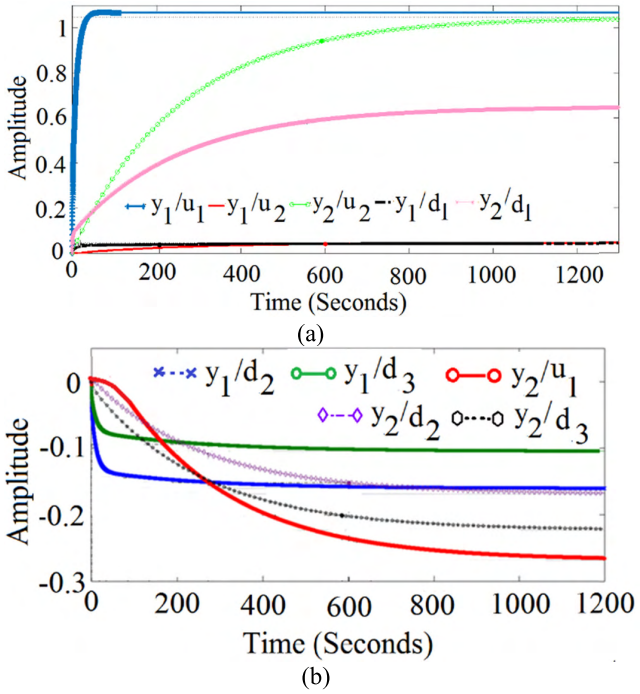

FIGURE 6. Step response of the simulated model transmittances a) y_1/u_1 in blue line, y_1/u_2 in red line, y_1/d_1 in black line, y_2/u_2 in bottle green line and y_2/d_1 in pink line b) y_2/u_1 in red line, y_1/d_2 in blue line, y_1/d_3 in green line, y_2/d_2 in purpel line and y_2/d_3 in black line.

where y_m denotes the measured output, y_{sim} represents the simulated output and $\overline{y_m}$ is the mean of measured output. The statistical coefficien indicates how well the model output fit to the plant output and must be close to 1. The coefficient-of-determination (R_T^2) were computed for the outputs ($y_1(k)$, $y_2(k)$) and found to be reasonably accurate such as 0.993 and 0.986 respectively.

B. CONTROL DESIGN

With the available accurate digital model, the proposed SSMPC based controller was applied on the simulated model, thereafter it has been applied to the actual experimental model, with the help of PLC HC900. In this section, the results obtained from the simulated control system are presented; thereafter experimental results are presented and compared with conventional PID control system. The design were carried out in the presence of three different types of input and output constraints such as amplitude and incremental variation constraints imposed on control variables $u(k)$ and amplitude constraints on output variables $y(k)$. The constrained on control variable $u_1(k)$ and the corresponding incremental variation $\Delta u_1(k)$ are chosen in such a way so that the drying materials can attain a sustained conveyance and at the same time it ensures to provide an adequate drying time. Therefore the speed of blower motor-drive was adjusted in the range between 40% - 70% of rated speed (1500 *rpm*). Similarly the constraints on control variable $u_2(k)$ and the corresponding incremental variation $\Delta u_2(k)$ are considered according to the material throughputs and initial moisture content of wet materials, so the drying materials get properly dried. Considering these facts, air inlet heat flow rate has been adjusted between 47% - 90% of maximum heat inflow rate (208, 800 KJ/h). On the other hand the hard amplitude constraints on outputs are taken according to the minimum and maximum values of respective set-point signals computed by the temperature drop model for a known drying condition. However in design the hard constraints imposed on output variables were soften by choosing a large slack variable (s_v) in order to avoid the violation of input constraints caused due to the enforcement of output constraints. Based on the practical consideration of unit operations, these constraints are summarized as follows:

Constraint on control variables ($N(u_1)$, $\dot{q}(u_2)$

$$\begin{aligned} 600\ rpm &\le u_1(k) \le 1050rpm \quad \forall k \\ 27.2KJ/s &\le u_2(k) \le 52.2KJ/s \quad \forall k \\ -50rpm &\le u_1(k) - u_1(k-1) \le 50rpm \quad \forall k \\ -4.2KJ/s &\le u_2(k) - u_2(k-1) \le 4.2KJ/s \quad \forall k \end{aligned} \tag{45}$$

Constraint on outputs ($v_a(y_1)$ and $T_a(y_2)$)

$$\begin{aligned} 133.33\ m3/h &\le y_1(k) \le 328.35\ m3/h \quad \forall k \\ 50^\circ C &\le y_2(k) \le 120^\circ C \quad \forall k \end{aligned}$$

Simulation of Controlled Process: Considering the desired response time and computational complexity of the design predictive controller, the control horizon (N_c) and prediction horizon (N_p) are chosen as 4 and 20 samples respectively and initially the control interval (T_s) is taken as 5 seconds. The performance weight matrices of the cost function (see Appendix III) are chosen as $\overline{R} = 0.1I_{6\times6}$ and $\overline{R}_s = I_{10\times2}$ [65], [68], [71].

The control performance of the designed predictive controller is analyzed in closed-loop simulation and shown in Figure 7.

These simulations were carried out at different values of air flow ($r_1(k)$) and air temperature ($r_2(k)$) set points, strategically varied in between 133.33 $m3/h$ -328.35 $m3/h$ and 50°C -120°C respectively with the model parameter values as presented in Table II. Figure 7 panel (a) shows the tracking of air flow and temperature outputs $y_1(k)$, $y_2(k)$) with the corresponding set point ($r_1(k)$, $r_2(k)$) variations. The associated manipulated variable responses are presented in Figure 7 panel (b).The figure shows clearly the comportment of manipulated variables over an interval of 50 minutes in order to maintain the output responses at their respective set points.

The flow output ($y_1(k)$) is varied in accordance with the changes of control input $u_1(k)$ and independent of alteration of control input $u_2(k)$. On the other hand, the control input $u_1(k)$ has a substantial influence on prediction of temperature output ($y_2(k)$). It is seen from the Figure 7 (a), the instances where the process exhibits a flow set point change, a notable variation is observed in the temperature output response. It is also viewed from the Figure 7 (b), at the same instances, the control variable $u_2(k)$ increases or decreases accordingly

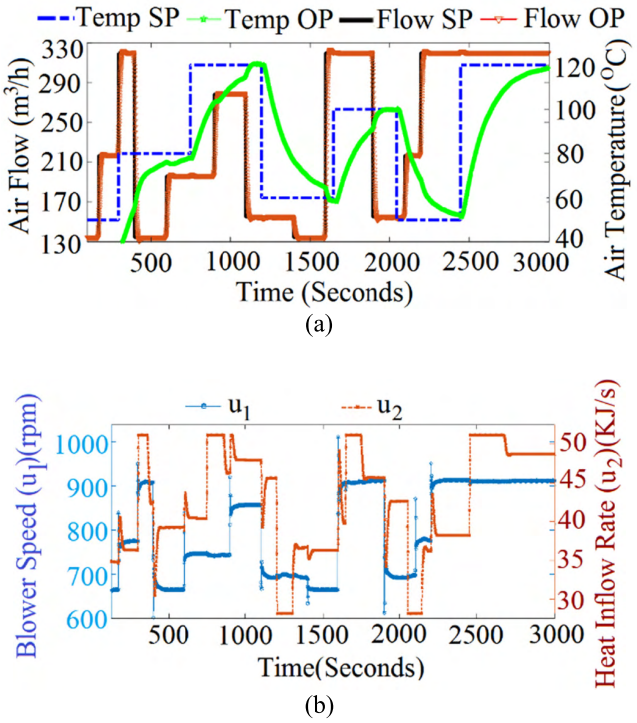

FIGURE 7. Closed-loop simulation of Pneumatic Conveying and Drying process with SSMPC control action (a) air flow and temperature outputs ($y_1(k), y_2(k)$) with the corresponding set point ($r_1(k), r_2(k)$ variations (b) manipulated variables: control input $u_1(k)$ and $u_2(k)$.

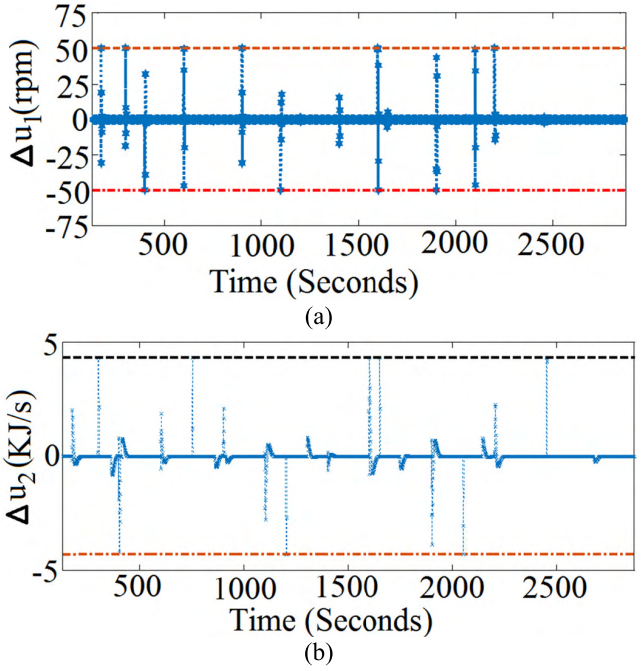

FIGURE 8. Rate of changes of manipulated variable response: (a) Δu_1 ($-50rpm \le u_1(k) - u_1(k-1) \le 50rpm$ (b)) Δu_2 ($-3.5KJ/sec \le u_2(k) - u_2(k-1) \le 3.5KJ/sec$).

in order to compensate the effect of control variable $u_1(k)$ on temperature output ($y_2(k)$). The tracking of air temperature in the process is much slower compared to air flow as because, the limited heating capacity of the preheating furnace imposes a hard constraint on control input $u_2(k)$ and corresponding increment Δu_2 which prevent the temperature output to grow faster nullifying the large time constants involve in air heating.

The rate of changes in manipulated variables Δu_1 and Δu_2 are plotted in Figure 8-panels *a* and *b* respectively. It is clearly seen from Figure 7 (b) and Figure 8, the control variables and their variation rates are within the specified limits as in (45).

Further to examine the performance of the controlled process at a selected drying condition ($M_0 = 0.2727$ kg-water/kg-dried solids and $M_f = 0.1256$ kg-water/kg-dried solids) for batch drying operation of rice powder material, some simulation studies were performed using a set of dynamic set points estimated by temperature drop model. On the basis of experimental results the best fitted empirical temperature drop model is estimated as

$$M_f = M_0 - 4.4286\,[T_a - T_{amb}]^{0.204} - 33.371 v_a^{-0.8} \quad (46)$$

At first the air flow set points are obtained using (8) for known dryer dimension and various parameter values as given in Table 2, then the required air temperature set points are determined using (46). Now, the performance of the predictive controller at some of the set points were studied in different control interval and the results are reported in Table 4. The energy cost for air heating and air flow are calculated as follows:

Energy cost of air heating:

$$J_H = \int_0^t u_2 dt = \sum_{i=1}^{NT_s} u_2(i) \quad (47)$$

Energy cost of air flow:

$$J_F = \sum_{i=1}^{NT_s} \frac{1}{2} \rho_a y_1(i) [v_a(i)]^2, \quad (48)$$

where time t = NT_s, N = number of samples and T_s is the control interval, y_1 = air flow output or volumetric flow rate in m^3/h, ρ_a is the air density. Now to find the correlation in between air velocity (v_a) in m/s and blower speed (u_1) in *rps*, a test has been conducted with the experimental setup under no load condition by keeping flow PID in manual mode. And finally, the correlation is obtained as

$$v_a = 0.0001428 u_1^2 + 0.1173 u_1 - 1.767 \quad (49)$$

For calculating the different performance indices in each case, the air flow and temperature set points have been changed at the same time instant from the same initial values 131.33 m^3/h and 50°C respectively and energy cost function is computed for the same duration (10 minutes).

It is seen from the results as obtained in Table 4, with the increase of temperature and flow set points for the same control interval the total energy cost of air and rise time for both air flow and air temperature are increased. On the

TABLE 4. Performance measures of controlled pneumatic conveying and drying process in different control interval.

Drying Conditions for M_0=27.27%$_{dB}$ and M_f=12.56%$_{dB}$			Performance Measures											
			Energy cost of air ($J_a = J_F + J_H$)						Rise time (t_r) (0-100%)					
Air Temp T_a (o_C)	Air Flow Rate V_a (m/s)	Air Flow (m^3/h)	J_F (KJ)			J_H(KJ)			(y_1) (Seconds)			(y_2) (Seconds)		
			T_s=5	T_s=20	T_s=40	T_s=5	T_s=20	T_s=40	T_s=5	T_s=20	T_s=40	T_s=5	T_s=20	T_s=40
71	10.09	165.65	0.936	0.926	0.841	3599	908.3	461.8	7	49	123	117	184	239
83	11.42	187.48	1.522	1.496	1.481	4262	1072	541.2	7	62	154	167	224	287
87	11.85	194.53	1.773	1.719	1.638	4473	1124	566.2	7	79	162	186	242	304
92	12.48	205.08	2.108	2.061	2.032	4733	1187	597.9	7	86	189	212	269	317
102	13.66	224.25	2.982	2.893	2.841	5225	1307	656.1	7	123	212	274	329	375
109	14.55	238.86	3.749	3.612	3.536	5586	1384	693.1	7	151	246	330	387	436
116	15.44	253.47	4.637	4.427	4.317	5830	1455	726.6	8	182	306	398	456	502
119	15.91	261.20	5.160	4.907	4.740	5944	1482	740.1	9	199	314	440	496	541

other hand with the increase of control interval (T_s) of the predictive controller for each set point, the total energy cost of air decreases but the rise time of air flow and air temperature responses have been increased significantly. For instance, at set point (119 $^\circ C$, 260.2 m^3/h) for the increase of control interval from 5 seconds to 20 seconds the rise time of air flow is increased to 22.11 times but for the variation from 20 seconds to 40 seconds it has been increased to only 1.58 times. Further it can be observed that for the increase of control interval from 5 seconds to 20 seconds the average energy cost of air for different set point is reduced to 74.88% but for the variation from 20 seconds to 40 seconds the average energy cost has been reduced to only 49.5%. The study reveals that the selection of larger control interval would increase the energy efficiency of the dryer to a large extent, but it would make the air flow and temperature responses more sluggish. Thus to select the control interval of the predictive controller, there should be a proper tradeoff between energy cost and response time of the air flow and temperature responses. Considering these facts, the control interval of the predictive controller for further simulation and experimental study has been chosen as 20 seconds.

However the relatively sluggish air flow and temperature responses obtained at the starting instant does not have any significant effect on drying performance and product quality, as because the process under investigation is engaged with a continuous batch drying operation. From the point of view of an efficient dryer operation, the measure of disturbance recovery time (t_{dr}) for material throughput alteration or initial moisture variation and the corresponding loss of product quality and total energy cost for a considerable period of operation would be more relevant than estimating performance measures at starting instant. The loss of product quality caused by material throughput variation can be defined in terms of mean deviation in material moisture from its desired or target moisture value (within $\pm 1\%$ tolarences) and given by

$$Q_L(in\%) = \frac{\sum_{i=1}^{NT_s} |M(i) - M_f|}{NT_s \times M_f} \times 100 \qquad (50)$$

where, N= number of samples and T_s is the control interval, $M(i)$ = final material moisture at i^{th} time instant and M_f = desired final moisture.

Now the various performance indices such as disturbance recovery time (t_{dr}) of air flow and temperature responses, total energy cost of air (J_a), loss of product quality (Q_L) of controlled process were estimated for $\pm 25\%$ variation of material feeding rate $(\dot{m}_p)$ from its nominal operating value (*20 kg-wet solid/s/m*^{2}). All the performance measures have been computed for the same duration of dryer operation (approximately 12 minutes excluding the set point alteration period) at different drying conditions (air temperature and flow set points) but varied from same initial values: 131.33 m^3/h and 50$^\circ C$ respectively with control interval of 20 seconds. The obtained results are presented in Table 5.

The study clearly indicates the disturbance recovery time for both air flow and temperature responses have a high correlation with the set point and material throughput alterations such that the disturbance recovery time for the responses get reduced or increased in accordance with the intensification of corresponding set points while the material feeding rate has been altered to 15 *kg-wet solid/s/m*^{2} and 25 *kg-wet solid/s/m*^{2} respectively. Subsequently, the product quality loss Q_{L_n} (or Q_{L_p}) estimated for any drying conditions proportionately varies with the corresponding disturbance recovery time of air flow and temperature responses. On the other hand, the total energy cost of air is increased for both positive and negative alteration of material throughputs with the increase of air temperature and flow set points.

Further with the variance of set points, similar type of trends are observed for the total energy cost and product quality loss when the process is subjected to a negative alteration of material feeds, whereas an opposite type of tendency is perceived in the presence of positive disturbances, which leads to an optimization problem. The optimal set point for dryer operation can be obtained by minimizing the objective function

$$J_{opt} = \sum_{j=1}^{N_{OP}} \left[\Lambda_0 \left(J_{a_n} + J_{a_p}\right) + \Lambda_1 Q_{L_n} + \Lambda_2 Q_{L_p}\right], \qquad (51)$$

TABLE 5. Performance measures of controlled pneumatic conveying and drying process with material throughput alteration.

Drying Conditions for M_0=27.27%$_{dB}$ and M_f=12.56%$_{dB}$		Performance Measures: Negative disturbance (-25% $\dot{m}_p$variation) $\dot{m}_p$=15 *kg-wet solid/s/m*^{2}				Positive disturbance (+25% $\dot{m}_p$variation) $\dot{m}_p$=25 *kg-wet solid/s/m*^{2}			
Air Temp T_a (^OC)	Air Flow (m^3/h)	Total energy cost of air (J_{a_n}) (KJ)	Loss of product quality (Q_{L_n}) (in %)	Disturbance recovery time (t_{dr}) (Seconds)		Total energy cost of air (J_{a_p}) (KJ)	Loss of product quality (Q_{L_p}) (in %)	Disturbance recovery time (t_{dr}) (Seconds)	
				Air flow response	Air temperature response			Air flow response	Air temperature response
71	165.65	306.6	1.954	94	240	866.8	0.979	33	123
83	187.48	366.3	1.409	81	160	929.9	1.070	38	132
87	194.53	386.5	1.227	78	150	951	1.103	47	143
92	205.08	412.4	1.080	66	135	978.8	1.175	65	147
102	224.25	464.8	0.845	53	111	1030.5	1.462	74	178
109	238.86	502.6	0.751	51	109	1065.1	1.771	85	217
116	253.47	539.7	0.758	47	113	1095.8	2.572	125	311
119	261.20	556.5	0.749	42	105	1126.3	3.428	159	396

where N_{OP} is the number of set points or drying conditions obtained through temperature drop model, Λ_0, Λ_1 and Λ_2 are the death penalties associated with the cost functions $J_{a_n}+J_{a_p}$, Q_{L_n} and Q_{L_p} respectively. As per the requirement of the optimization problem, penalties Λ_1 and Λ_2 were simply chosen as large as 1.39e5 and 1e5 respectively and a comparatively lower weight (1e2) has been selected for the penalty associated with the total air energy cost function.

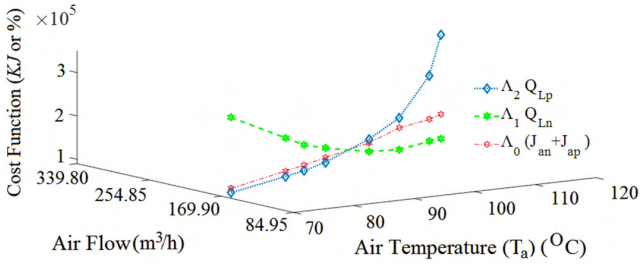

FIGURE 9. Optimal set point estimation through optimization.

Figure 9 shows the variation of the various cost indices of the objective function (J_{opt}) with the corresponding changes in air flow and temperature set points. The plot clearly shows, the possible solution of the optimal set point detection problem is located at the intersecting point and consequently where the air flow and temperature set points are varied near 205.09 m^3/h and 92 $^\circ C$ respectively. Thus, to achieve an economic drying performance and a satisfactory product quality for the rice powder materials, the optimal air temperature and air flow set points of dryer operation are set to be 92 $^\circ C$ and 205.09 m^3/h respectively.

Figure 10 shows the set point tracking and compensation of measured disturbances (material feed alteration) of the simulated controlled process. To obtain the responses air flow and temperature set points were varied to the optimal

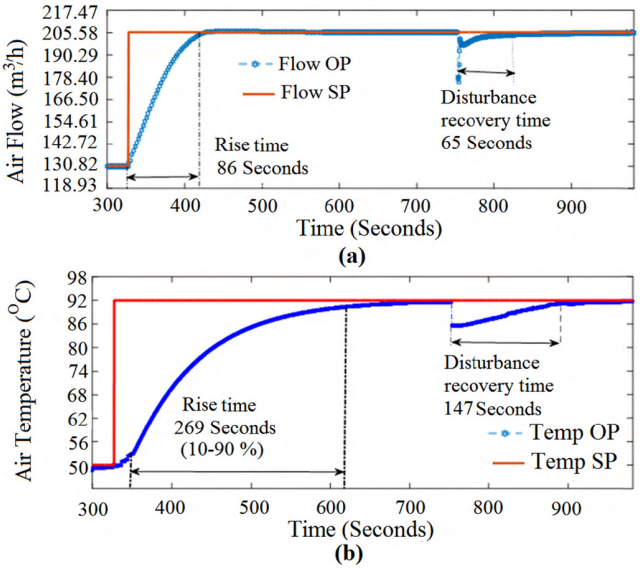

FIGURE 10. Simulated response of the controlled process with +25% material throughput alterations: (a) air flow response (b) air temperature response.

setting (92 $^\circ C$ and 205.09 m^3/h respectively) from the initial values (50 $^\circ C$ and 131.33 m^3/h respectively) at the same time instant (320 seconds) with a material feeding rate of 20 *kg-wet solid/s/m*2.

Then at 720 seconds, material throughput has been altered to 25 *kg-wet solid/s/m*^{2}. The various tracking performance measures for the air flow and temperature responses were found to be rise time: 86 seconds and 269 seconds, steady state error: NIL and % peak overshoot: 0.062% and 0% respectively. The disturbance recovery times for both the responses were measured as 65 seconds and 147 seconds respectively. It is generally agreed that the air temperature

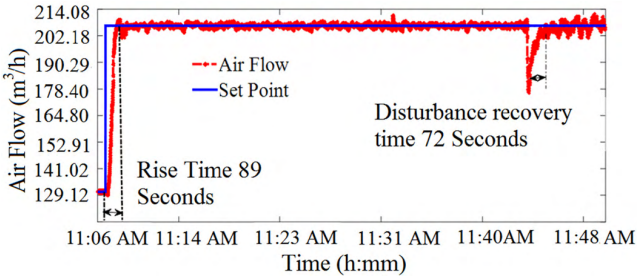

FIGURE 11. Experimental air flow response of the proposed SSMPC controller implemented in LabVIEW real time environment through PLC mod-bus interface.

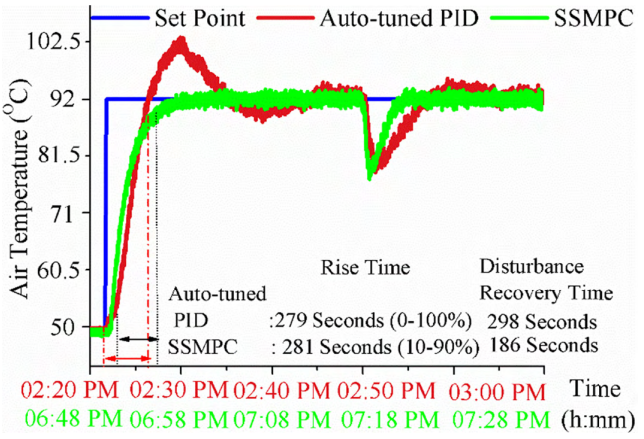

FIGURE 12. Comparison of drying performance (air temperature response) of proposed SSMPC controller and auto-tuned PID controller of HC900 PLC. (Time axis is shown in red and green color for Auto-tuned PID and SSMPC respectively.

response of the electrically heated pneumatic dryers are much slower than the gas or oil fired dryers, but a proper design and implementation of predictive control with prior knowledge of process models can reduce the air temperature response time significantly, thus reduces the total energy cost of air and product quality loss, which certainly improves the overall efficiency of the dryer and product quality.

Experiments on Controlled Process: The main goal of performing system identification and control design was to implement and test the SSMPC strategy on the real pneumatic conveying and drying process involves with the batch processing of rice powder materials for a known drying condition. To examine the dryer performance under practical setting, the developed predictive control law was implemented in LabView 72] real time environment through a PLC mod bus interface. To perform the experiment,at first the experimental setup was run under no-load for more than one hour with a fixed temperature setting of 50 $^{\circ}C$ and flow setting of 131.33 m^3/h, then the rice powder material was fed into the hopper at a feeding rate of 20 *kg-wet solid/s/*m^2 by means of feed control valve. As soon as the air flow and temperature responses settled down, the air temperature and flow set points were changed to 92 $^{\circ}C$ and 205.09 m^3/h respectively. Then, approximately after 33 minutes of dryer operation the rate of rice powder feed was changed to 25 *kg-wet solid/s/*m^2. A section of the air flow response of the experimental controlled process is presented in Figure 11.

From the figure, the various performance indices of the air flow response such as rise time, peak overshoot, steady state error, disturbance recovery time were measured and found to be 89 seconds, 0.102%, 0.521% and 72 seconds respectively. The study clearly demonstrates that measured performance indicators are reasonably correct and closely correlated with the indices estimated from simulation study (see Figure 10(a)). In order to compare the drying performance of the proposed SSMPC controller against a conventional controller, another set of experiments were performed with similar type of set point and material throughput alteration and operating and environmental conditions, with the auto-tuned PID controller of HC900 PLC and proposed SSMPC controller respectively, and the comparative results of air temperature response for a considerable duration is presented in Figure 12. It is observed from the figure, the rise time of auto-PID controller (279 seconds) is slightly less than that of proposed controller (281 seconds), but auto-tuned PID exhibits approximately 11.41% peak overshoot during set point alteration compared to zero overshoot in proposed control action. The study gives an indication that the product quality of the dryer with inbuilt PID controller may degrade if any set point alteration occurs during batch operation of the dryer.

Again, it can be seen from the figure the steady state error of the proposed control action is much less than that of auto-tuned PID controller. In terms of disturbance rejection the proposed controller can perform in a better way compared to the auto-tuned PID controller. The disturbance recovery time for the material throughput alteration were measured from the corresponding air temperature responses of auto-tuned PID and proposed controller, and found to be 298 seconds and 186 seconds respectively. Therefore, it can be stated that the proposed controller can provide much better drying performance compared to the exiting auto-tuned PID controller. Further to examine the improvement of product quality in proposed control action over the inbuilt auto-tuned PID, the product quality loss has been computed for the same duration (approximately 48 minutes as shown in Figure 12) and found to be 6.34% and 14.83% respectively. Thus, the implementation of proposed SSMPC controller has reduced the product quality loss by 57.25% and hence improved the product quality by 9.97% compared to the inbuilt auto-tuned PID controller.

Moreover to investigate the performance and accuracy of the soft sensor in measuring the powder material moisture online, a series of tests on the controlled process have been conducted batch-wise using the same rice powder material (moisture conditioned at 0.2727 kg-water/kg-dried solids (27.27%)) and drying condition (set points: 92 $^{\circ}C$ and 205.09 m^3/h, at material feeding rate o 20 *kg-wet solid/s/*m^2. The target moisture of the rice powder has been set to 12.56% in order to acquire the properly dried material and

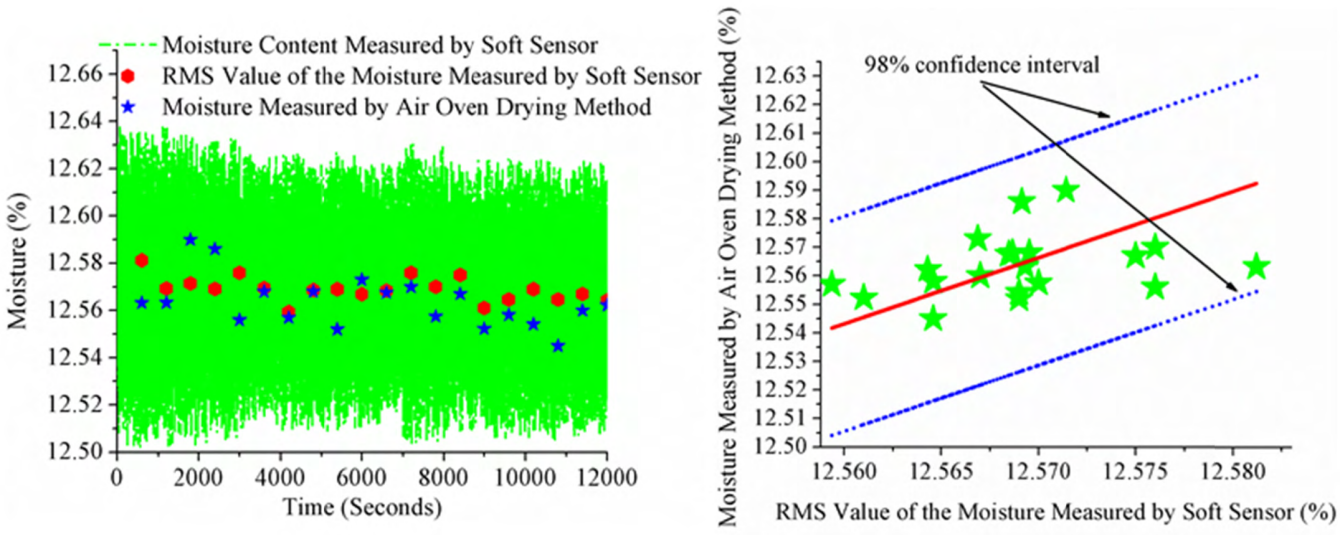

(a) (b)

FIGURE 13. Comparison between moisture measured by soft sensor and air oven drying method.

maintaining the product quality. The dried rice power materials at cyclone were collected in separate plastic bags for every 10 minutes operation of the dryer. Then the final moisture contents were measured using 10g samples of each plastic bag by an air-oven drying method (131.15 $^{\circ}C$, 24h) one after another. The responses of the soft sensor during the tests were also captured and the *rms* values of moisture measurements have been computed for every 10 minutes interval. Figure 13(a) shows a comparative study of moisture measurements measured using the developed soft sensor and air oven drying method. The correctness of the measurement is further investigated in Figure 13(b). It can be seen from Figure 13(b) that the measured moistures by soft sensor (rms value) and air oven drying method were in a reasonable agreement (within 98% confidence interval) with each other. The study also affirms the benefits of using the soft sensor in measuring the powder material moisture replacing the costly online moisture meters.

VI. CONCLUSIONS

The paper has presented the modeling, identification and control of pneumatic conveying dryer involves with the batch processing of powder materials by using first principle's, system identification techniques and a predictive control approach in a systematic manner. The alternative predictive drying control framework employed in this paper; invalidate the compulsion of using costly, inaccurate online solid moisture measurement sensors in implementing any automated drying control system. The work presented in this contribution has developed a novel control oriented first principle's model of the pneumatic conveying and drying system in the state space form. Then the parameters of first principle's model have been identified in the structured form by using refined PSO based model structured parameter identification method which is being proposed and developed in this contribution. The modeling strategies adopted in this paper also address how control-oriented modeling of complex systems can benefit from integrating first principle's and system identification methods. The work has evolved an online drying condition detection scheme by designing a solid moisture soft sensor (temperature drop model) and an optimizer, which enables the determination of optimal air flow and dryer temperature working set points from the prior knowledge of the initial and target moisture of the processing material for each batch of production. The predictive control law proposed and developed on the basis of linearized multivariable model, stringent design specifications and dynamic operation conditions of the pneumatic conveying dryer, has shown its competence in tracking set point signals and satisfying various quantitative and qualitative indices related to drying performance and product quality. Finally, the developed control strategy has been implemented and tested under practical settings and affirmed its effectiveness in improving the drying performance and product quality compared to an inbuilt auto-tuned PID controller of Honeywell make HC900 PLC.

APPENDIX I

$$\dot{v_p} = \frac{A'_p}{2Vol_p} C_d \left(v_a - v_p\right)^2 \frac{\rho_a}{\rho_p} - \left(1 - \frac{\rho_a}{\rho_p}\right) g - \frac{f_p}{2D_{pipe}} v_p^2 \tag{a}$$

$$\dot{v}_a = \frac{A^2_{blower}}{A^2_{blower} + k_8} \left[-\psi \left(\frac{\pi D_{tip}}{60}\right)^2 N\dot{N} - g - \frac{2}{D_{pipe}} f_a v_a^2 - \frac{A'_p}{2Vol_p}\phi \right.$$

$$\times \frac{\rho_a v_a \left[1+M_0+k_3\left[T_a-T_{amb}\right]^{\gamma}+k_4/\left(\dot{m}_p\right)^{\eta}\right]}{\rho_p v_p \left[1-\phi\left[M_0+k_3\left[T_a-T_{amb}\right]^{\gamma}+k_4/\left(\dot{m}_p\right)^{\eta}\right]+\aleph\right]} \times C_d\left(v_a-v_p\right)^2+\phi\frac{v_a}{v_p}\left[v_a-v_p\right] \times \frac{\left[k_3\gamma\left[T_a-T_{amb}\right]^{\gamma-1}-\eta k_4/(\dot{m}_p)^{\eta+1}\right]}{\left[1-\phi[M_0+k_3[T_a-T_{amb}]^{\gamma}+k_4/(\dot{m}_p)^{\eta}]+\aleph\right]}\Bigg] \quad \text{(b)}$$

$$\dot{T}_p = \frac{A'_p}{c_p\rho_p Vol_p}h_{ap}\left(T_a-T_p\right) +\frac{1}{c_p}\frac{\left[k_3\gamma\left[T_a-T_{amb}\right]^{\gamma-1}-\eta k_4/\left(\dot{m}_p\right)^{\eta+1}\right]}{\left[1+M_0+k_3\left[T_a-T_{amb}\right]^{\gamma}+k_4/\left(\dot{m}_p\right)^{\eta}\right]} \times\left(k_6-k_7T_p\right)\left[1+\alpha e^{-\beta\left[M_0+k_3\left[T_a-T_{amb}\right]^{\gamma}+k_4/\left(\dot{m}_p\right)^{\eta}\right]}\right] \quad \text{(c)}$$

$$\dot{T}_a = -\frac{A'_p}{\rho_p C_a Vol_p}\phi \times\frac{v_a\left[1+M_0+k_3\left[T_a-T_{amb}\right]^{\gamma}+k_4/\left(\dot{m}_p\right)^{\eta}\right]}{v_p\left[1-\phi\left[M_0+k_3\left[T_a-T_{amb}\right]^{\gamma}+k_4/\left(\dot{m}_p\right)^{\eta}\right]+\aleph\right]}\dot{q} -\phi\frac{\dot{\S}}{C_a\dot{m}_p\left[1-\phi\left[M_0+k_3\left[T_a-T_{amb}\right]^{\gamma}+k_4/(\dot{m}_p)^{\eta}\right]+\aleph\right]} +\phi\frac{C_v v_a}{C_a v_p}\left(T_a-T_p\right) \times\frac{\left[k_3\gamma\left[T_a-T_{amb}\right]^{\gamma-1}-\eta k_4/\left(\dot{m}_p\right)^{\eta+1}\right]}{\left[1-\phi\left[M_0+k_3\left[T_a-T_{amb}\right]^{\gamma}+k_4/\left(\dot{m}_p\right)^{\eta}\right]+\aleph\right]} \quad \text{(d)}$$

APPENDIX II

$$A_\theta:\begin{bmatrix}0.3085 & -0.3477 & -0.0087 & 0\\ -0.2826 & 0.7486 & 0 & 0\\ -0.1007 & -0.0964 & 0.5919 & -0.1443\\ 0 & 0 & -0.7138 & 0.7415\end{bmatrix}$$

$$B_{u_\theta}:\begin{bmatrix}0.9616 & 0\\ 0 & 0\\ 0 & -0.3593\\ 0 & 0\end{bmatrix}$$

$$B_{d_\theta}:\begin{bmatrix}0.1890 & -0.0860 & -0.0666\\ 0 & 0 & 0\\ -0.3118 & -0.4974 & -0.1572\\ -0.1310 & -0.4972 & -0.2235\end{bmatrix}$$

$$C_\theta:\begin{bmatrix}0.3673 & 0 & 0 & 0\\ 0 & 0 & -0.0502 & 0\end{bmatrix}$$

APPENDIX III

The cost function [65]

$$J = \left[R_s - Fx_{Au}(k)\right]^T\left[R_s - Fx_{Au}(k)\right] + \Delta U^T\left[\Phi^T\Phi+\overline{R}\right]\Delta U - 2\Delta U^T\Phi^T\left[R_s - Fx_{Au}(k)\right] \quad \text{(e)}$$

Subjected to inequality constraints $M\Delta U \le \gamma$

Where F and Φ are the corresponding matrices of the predicted output combining one step to N_p step ahead predictions on the basis of augmented state space model written in the compact form [65], the matrix $\Phi^T\Phi$ has dimension $2N_c \times 2N_c$, $\Phi^T F$ has dimension $2N_c \times 6$, $R_s = [I]_{N_p\times 2}\, r(k)_{2\times 1}$, and $\Phi^T\Phi + \overline{R}$ is a positive definite Hessian matrix. The weight matrix $\overline{R}$ is a block matrix with 2 blocks and has its dimension equal to the dimension of $\Phi^T\Phi$. M is a matrix reflecting the constraints, with its number of rows equal to the number of constraints and the number of columns equal to the dimension of control effort (ΔU).

REFERENCES

[1] A. S. Mujumdar, Ed., *Handbook of Industrial Drying*. Boca Raton, FL, USA: CRC Press, 2014.
[2] B. Satpati, C. Koley, and S. Datta, "Modeling identification and control of an air preheating furnace of a pneumatic conveying and drying process," *Ind. Eng. Chem. Res.*, vol. 53, no. 51, pp. 19695–19714, 2014.
[3] B. Satpati, C. Koley, and S. Datta, "Online estimation of rice powder moisture in a pneumatic conveying dryer," in *Proc. IEEE Int. Conf. Circuit, Power Comput. Technol. (ICCPCT)*, 2016, pp. 1–6.
[4] D. Mills, *Pneumatic Conveying Design Guide*. London, U.K.: Butterworth, 2003.
[5] H. Holmberg and P. Ahtila, "Simulation model for the model-based control of a biofuel dryer at an industrial combined heat and power plant," *Drying Technol.*, vol. 24, no. 12, pp. 1547–1557, 2006.
[6] P. Dufour, "Control engineering in drying technology: Review and trends," *Drying Technol.*, vol. 24, no. 7, pp. 889–904, 2006.
[7] J. W. Robinson, "Improve dryer control," *Chem. Eng. Prog.*, vol. 88, pp. 28–33, Dec. 1992.
[8] C. Fyhr and A. Rasmuson, "Mathematical model of a pneumatic conveying dryer," *AIChE J.*, vol. 43, no. 11, pp. 2889–2902, 1997.
[9] R. D. Radford, "A model of particulate drying in pneumatic conveying systems," *Powder Technol.*, vol. 93, no. 2, pp. 109–126, 1997.
[10] A. H. Pelegrina and G. H. Crapiste, "Modelling the pneumatic drying of food particles," *J. Food Eng.*, vol. 48, no. 4, pp. 301–310, 2001.
[11] F. Tanaka, T. Uchino, D. Hamanaka, and G. G. Atungulu, "Mathematical modeling of pneumatic drying of rice powder," *J. Food Eng.*, vol. 88, no. 4, pp. 492–498, 2008.
[12] C. P. Narimatsu, M. C. Ferreira, and J. T. Freire, "Drying of coarse particles in a vertical pneumatic conveyor," *Drying Technol.*, vol. 25, no. 2, pp. 291–302, 2007.
[13] Z. Mindziul and A. Kmieć, "Modelling gas-solid flow in a pneumatic-flash dryer," *Drying Technol.*, vol. 15, nos. 6–8, pp. 1711–1720, 1997.
[14] M. Aghbashlo, S. Hosseinpour, and A. S. Mujumdar, "Application of artificial neural networks (ANNs) in drying technology: A comprehensive review," *Drying Technol.*, vol. 33, no. 12, pp. 1397–1462, 2015.
[15] U. Yuzgec, Y. Becerikli, and M. Turker, "Dynamic neural-network-based model-predictive control of an industrial baker's yeast drying process," *IEEE Trans. Neural Netw.*, vol. 19, no. 7, pp. 1231–1242, Jul. 2008.
[16] J. A. Hernández-Pérez, M. A. García-Alvarado, G. Trystram, and B. Heyd, "Neural networks for the heat and mass transfer prediction during drying of cassava and mango," *Innov. Food Sci. Emerg. Technol.*, vol. 5, no. 1, pp. 57–64, 2004.
[17] N. Perrot, C. Bonazzi, and G. Trystram, "Application of fuzzy rules-based models to prediction of quality degradation of rice and maize during hot air drying," *Drying Technol.*, vol. 16, no. 8, pp. 1533–1565, 2007.
[18] X. Liu, X. Chen, W. Wu, and G. Peng, "A neural network for predicting moisture content of grain drying process using genetic algorithm," *Food Control*, vol. 18, no. 8, pp. 928–933, 2007.
[19] U. Yuzgec, Y. Becerikli, and M. Turker, "Nonlinear predictive control of a drying process using genetic algorithms," *ISA Trans.*, vol. 45, no. 4, pp. 589–602, 2006.
[20] H. Abukhalifeh, R. Dhib, and M. Fayed, "Model predictive control of an infrared-dryer," in *Proc. IEEE Int. Conf. Phys. Control*, vol. 1. Aug. 2003, pp. 340–344.
[21] H. Abukhalifeh, R. Dhib, and M. E. Fayed, "Model predictive control of an infrared-convective dryer," *Drying Technol.*, vol. 23, no. 3, pp. 497–511, 2005.

[22] P. Dufour, Y. Touré, D. Blanc, and P. Laurent, "On nonlinear distributed parameter model predictive control strategy: On-line calculation time reduction and application to an experimental drying process," *Comput. Chem. Eng.*, vol. 27, no. 11, pp. 1533–1542, 2003.

[23] N. Daraoui, P. Dufour, H. Hammouri, and A. Hottot, "Model predictive control during the primary drying stage of lyophilisation," *Control Eng. Pract.*, vol. 18, no. 5, pp. 483–494, 2010.

[24] H. Didriksen, "Model based predictive control of a rotary dryer," *Chem. Eng. J.*, vol. 86, no. 1, pp. 53–60, 2002.

[25] I. C. Trelea, G. Trystram, and F. Courtois, "Optimal constrained non-linear control of batch processes: Application to corn drying," *J. Food Eng.*, vol. 31, no. 4, pp. 403–421, 1997.

[26] H. E. Musch, G. W. Barton, T. A. G. Langrish, and A. S. Brooke, "Non-linear model predictive control of timber drying," *Comput. Chem. Eng.*, vol. 22, no. 3, pp. 415–425, 1998.

[27] Q. Liu and F. W. Bakker-Arkema, "A model-predictive controller for grain drying," *J. Food Eng.*, vol. 49, no. 4, pp. 321–326, 2001.

[28] L. Zhang, H. Cui, H. Li, F. Han, Y. Zhang, and W. Wu, "Parameters online detection and model predictive control during the grain drying process," *Math. Problems Eng.*, vol. 2013, May 2013, Art. no. 924698.

[29] R. A. Bartlett, L. T. Biegler, J. Backstrom, and V. Gopal, "Quadratic programming algorithms for large-scale model predictive control," *J. Process Control*, vol. 12, no. 7, pp. 775–795, 2002.

[30] C. Karthik, K. Valarmathi, and M. Rajalakshmi, "Nonlinear modeling of moisture control of drying process in paper machine," *Procedia Eng.*, vol. 38, pp. 1104–1111, 2012.

[31] R. Arjona, P. Ollero, and F. Vidal-Barrero, "Automation of an olive waste industrial rotary dryer," *J. Food Eng.*, vol. 68, no. 2, pp. 239–247, 2005.

[32] P. Dufour, D. Blanc, Y. Touré, and P. Laurent, "Infrared drying process of an experimental water painting: Model predictive control," *Drying Technol.*, vol. 22, nos. 1–2, pp. 269–284, 2004.

[33] C. Bordons and A. Núñez-Reyes, "Model based predictive control of an olive oil mill," *J. Food Eng.*, vol. 84, no. 1, pp. 1–11, 2008.

[34] J. De Temmerman, P. Dufour, B. Nicolaï, and H. Ramon, "MPC as control strategy for pasta drying processes," *Comput. Chem. Eng.*, vol. 33, no. 1, pp. 50–57, 2009.

[35] F. B. Freire, G. N. A. Vieira, J. T. Freire, and A. S. Mujumdar, "Trends in modeling and sensing approaches for drying control," *Drying Technol.*, vol. 32, no. 13, pp. 1524–1532, 2014.

[36] P. Kadlec, B. Gabrys, and S. Strandt, "Data-driven soft sensors in the process industry," *Comput. Chem. Eng.*, vol. 33, no. 4, pp. 795–814, Apr. 2009.

[37] R. K. Shah and D. P. Sekulic, *Fundamentals of Heat Exchanger Design*. Hoboken, NJ, USA: Wiley, 2003.

[38] K. S. Rajan, K. Dhasandhan, S. N. Srivastava, and B. Pitchumani, "Studies on gas–solid heat transfer during pneumatic conveying," *Int. J. Heat Mass Transf.*, vol. 51, nos. 11–12, pp. 2801–2813, 2008.

[39] M. Ellis, H. Durand, and P. D. Christofides, "A tutorial review of economic model predictive control methods," *J. Process Control*, vol. 24, no. 8, pp. 1156–1178, 2014.

[40] T. Backx, O. Bosgra, and W. Marquardt, "Integration of model predictive control and optimization of processes," in *Proc. IFAC Symp. Adv. Control Chem. Process.*, 2000, pp. 249–260.

[41] J. J. Siirola and T. F. Edgar, "Process energy systems: Control, economic, and sustainability objectives," *Comput. Chem. Eng.*, vol. 47, pp. 134–144, Dec. 2012.

[42] C. Altafini and M. Furini, "Robust control of a flash dryer plant," in *Proc. IEEE Int. Conf. Control Appl.*, 1997, pp. 785–787.

[43] P. Bunyawanichakul, G. J. Walker, J. E. Sargison, and P. E. Doe, "Modelling and simulation of paddy grain (rice) drying in a simple pneumatic dryer," *Biosyst. Eng.*, vol. 96, no. 3, pp. 335–344, 2007.

[44] D. B. Brooker, F. W. Bakker-Arkema, and C. W. Hall, *Drying and Storage of Grains and Oilseeds*. Springer, 1992.

[45] C. Laithong, "Study of thermo-physical properties of rough rice," M.S. thesis, Faculty Energy Mater., King Mongkut's Inst. Technol. Ladkrabang, Bangkok, Thailand, 1987.

[46] W. Zhuang, V. N. M. Roderick, and F. Borup, "Model-based analysis and simulation of airflow control systems of ventilation units in building environments," *Building Environ.*, vol. 42, no. 1, pp. 203–217, Jan. 2007.

[47] P. Van Overschee and B. De Moor, *Subspace Identification for Linear Systems: Theory—Implementation—Applications*. Springer, 2012.

[48] L. Ljung and T. McKelvey, "Subspace identification from closed-loop data," *Signal Process.*, vol. 52, no. 2, pp. 209–215, 1996.

[49] G. Mercère, O. Prot, and J. A. Ramos, "Identification of parameterized gray-box state-space systems: From a black-box linear time-invariant representation to a structured one," *IEEE Trans. Autom. Control*, vol. 59, no. 11, pp. 2873–2885, Nov. 2014.

[50] L. Ljung, "Perspectives on system identification," *Annu. Rev. Control*, vol. 34, no. 1, pp. 1–12, 2010.

[51] L.-L. Xie and L. Ljung, "Estimate physical parameters by black box modeling," in *Proc. 21st Chin. Control Conf.*, 2002, pp. 673–677.

[52] H. Hjalmarsson, M. Gevers, and F. Bruyne, "For model based control design, closed loop identification gives better performance," *Automatica*, vol. 32, no. 12, pp. 1659–1673, 1996.

[53] P. Van den Hof, "Closed-loop issues in system identification," *Annu. Rev. Control*, vol. 22, pp. 173–186, 1998.

[54] U. Forssell and L. Ljung, "Closed-loop identification revisited," *Automatica*, vol. 35, no. 7, pp. 1215–1241, 1999.

[55] P. Van Overschee and B. De Moor, "Closed loop subspace system identification," in *Proc. 36th IEEE Conf. Decision Control*, vol. 2. Dec. 1997, pp. 1848–1853.

[56] Q. B. Jin, Z. J. Cheng, J. Dou, L. T. Cao, and K. W. Wang, "A novel closed loop identification method and its application of multivariable system," *J. Process Control*, vol. 22, no. 1, pp. 132–144, 2012.

[57] H.-F. Wang and H.-W. Hsu, "A closed-loop logistic model with a spanning-tree based genetic algorithm," *Comput. Oper. Res.*, vol. 37, no. 2, pp. 376–389, 2010.

[58] J. Kennedy, "Particle swarm optimization," in *Encyclopedia of Machine Learning*. New York, NY, USA: Springer, 2011, pp. 760–766.

[59] A. Alfi and H. Modares, "System identification and control using adaptive particle swarm optimization," *Appl. Math. Model.*, vol. 35, no. 3, pp. 1210–1221, 2011.

[60] D. Sendrescu, "Parameter identification of anaerobic wastewater treatment bioprocesses using particle swarm optimization," *Math. Problems Eng.*, vol. 2013, pp. 1–8, Jun. 2013.

[61] P. Kou, J. Zhou, C. Wang, H. Xiao, H. Zhang, and C. Li, "Parameters identification of nonlinear state space model of synchronous generator," *Eng. Appl. Artif. Intell.*, vol. 24, no. 7, pp. 1227–1237, 2011.

[62] Ö. Yeniay, "Penalty function methods for constrained optimization with genetic algorithms," *Math. Comput. Appl.*, vol. 10, no. 1, pp. 45–56, 2005.

[63] T. Bäck, F. Hoffmeister, and H.-P. Schwefel, "A survey of evolution strategies," in *Proc. 4th Int. Conf. Genetic Algorithms*, 1991, pp. 1–8.

[64] A. Homaifar, C. X. Qi, and S. H. Lai, "Constrained optimization via genetic algorithms," *Simulation*, vol. 62, no. 4, pp. 242–253, 1994.

[65] L. Wang, *Model Predictive Control System Design and Implementation Using MATLAB*. Springer, 2009.

[66] S. Li, K. Y. Lim, and D. G. Fisher, "A state space formulation for model predictive control," *AIChE J.*, vol. 35, no. 2, pp. 241–249, 1989.

[67] K. R. Muske and J. B. Rawlings, "Model predictive control with linear models," *AIChE J.*, vol. 39, no. 2, pp. 262–287, 1993.

[68] M. Ramzi, H. Youlal, and M. Haloua, "State space model predictive control of an aerothermic process with actuators constraints," *Intell. Control Autom.*, vol. 3, pp. 50–58, 2012.

[69] M. Deflorian and S. Zaglauer, "Design of experiments for nonlinear dynamic system identification," *IFAC Proc. Vol.*, vol. 44, no. 1, pp. 13179–13184, 2011.

[70] P. Bhattacharjee, R. S. Singhal, and P. R. Kulkarni, "Basmati rice: A review," *Int. J. Food Sci. Technol.*, vol. 37, no. 1, pp. 1–12, 2002.

[71] M. Morari and N. L. Ricker, *Model Predictive Control Toolbox: For Use With MATLAB*, MathWorks Inc., Natick, MA, USA, 1998.

[72] *The LabVIEW User Manual*, National Instrum., Austin, TX, USA, 1998.

BIPLAB SATPATI (M'08) was born in West Bengal, India. He received his Bachelor degree in electrical engineering from Bengal Engineering College, Shibpur in 2002. He obtained his Master of Engineering with specialization in control system engineering from Jadavpur University in 2007.

Presently he holds the post of Assistant Professor in the Department of Electrical Engineering, University Institute of Technology, The University of Burdwan, India. He is also working as a part-time research scholar in Electrical Engineering Department, National Institute of Technology, Durgapur. His area of interest is model based control design, robust and predictive control.

CHIRANJIBKOLEY (M'02) was born in West Bengal, India. He obtained his B.Tech, M.Tech, and Ph.D. degrees in 2000, 2002 and 2007, respectively.

Presently he holds the post of Associate Professor in the Department of Electrical Engineering, National Institute of Technology, Durgapur, India. He has published more than 20 research papers and developed an online course. His current research includes condition monitoring of electrical equipment, signal processing, machine learning, instrumentation and control.

SUBHASHIS DATTA was born in Burdwan, West Bengal, India. He obtained his B.Tech. and Ph.D. degrees in 2000 and 2008, respectively.

Presently he holds the post of Professor in the Department of Mechanical Engineering, Ghani Khan Choudhury Institute of Engineering and Technology, Malda, India. His current research includes pneumatic conveying and drying system, model based control design, robust and predictive control.